Catalytic Steam and Partial Oxidation Reforming of liquid fuels for application in improving the efficiency of internal combustion engines

D. William Brookshear, Josh A. Pihl, James P. Szybist*

Oak Ridge National Laboratory, Oak Ridge, TN 37831 United States

*Corresponding Author: Josh A. Pihl

pihlja@ornl.gov

1-865-946-1524

2360 Cherahala Blvd, Knoxville, TN 37932

Keywords: partial oxidation reforming, steam reforming, thermochemical recuperation,

Abstract

This study investigated the potential for catalytically reforming liquid fuels in a simulated exhaust gas recirculation (EGR) mixture loop for the purpose of generating reformate that could be used to increase stoichiometric combustion engine efficiency. The experiments were performed on a simulated exhaust flow reactor using a Rh/Al_2O_3 reformer catalyst, and the fuels evaluated included iso-octane, ethanol, and gasoline. Both steam reforming and partial oxidation reforming were examined as routes for the production of reformate. Steam reforming was determined to be an ineffective option for reforming in an EGR loop due to the high exhaust temperatures (in excess of 700 °C) required to produce adequate concentrations of reformate, regardless of fuel. However, partial oxidation reforming is capable of producing hydrogen concentrations as high as 10-16%, depending on fuel and operating conditions in the simulated EGR gas mixture. Meanwhile, measurements of total fuel enthalpy retention were shown to have favorable energetics under a range of conditions, although a tradeoff between fuel enthalpy retention and reformate production was observed. Of the three fuels evaluated, iso-octane exhibited the best overall performance, followed by ethanol and then gasoline. Overall, it was found that partial oxidation reforming of liquid fuels in a simulated EGR mixture over the Rh/Al_2O_3 catalyst demonstrated sufficiently high reformate yields and favorable energetics to warrant further evaluation in the EGR system of a stoichiometric combustion engine.

1. Introduction

Improving the efficiency of spark-ignited (SI) engines is desired as a way to help meet the challenging fuel economy and CO_2 emission regulations that are being phased-in around the world.[1] Cooled exhaust gas recirculation (EGR) has well-established thermodynamic benefits while maintaining a stoichiometric air-to-fuel ratio, allowing the mature three-way catalyst technology to be used for emissions control.[2] Additionally, EGR suppresses knock in SI engines, which enables further efficiency increases through more advanced combustion phasing or higher compression ratios.[3] However, the amount of EGR dilution that can be applied is limited because of cycle-to-cycle instability, the root cause of which is the reduction of flame speed with EGR.[4–9]

Due to its high flame speed, the addition of H_2 or H_2-rich reformate increases the combustion rate and can significantly extend the EGR dilution limit, resulting in improvements in engine efficiency.[10,11] The amount of H_2 required to achieve significant improvements depends on the specifics of the engine hardware and operating conditions. Alger et al. were able to increase the EGR dilution tolerance from 25% to 50% with only 1 vol% H_2 in the intake manifold.[10] In contrast, Fennell et al. were only able to increase the EGR dilution tolerance from 21% to 27% using 1.5 vol% H_2.[12] It should be noted that these concentrations are at the engine intake manifold; achieving these concentrations would require 2 to 3 times as much H_2 at the outlet of an EGR loop reforming catalyst due to dilution by incoming air in the intake manifold. This work focused on achieving H_2 concentrations of at least 5% in the reformer effluent. The optimal H_2 concentration will depend on the specifics of the combustion system and operating conditions as well as the energy balance across the reforming catalyst.

While the beneficial uses of H_2 are well established, efficient generation of H_2 from liquid fuel via a robust fuel reformation has proven difficult. Hwang et al. incorporated a catalytic fuel reformer system on a diesel engine, and while the reformer effluent had a H_2 concentration of more than 10%, there was an overall decrease in engine efficiency.[13] Ashida et al. incorporated steam reforming in an EGR-loop with a reforming catalyst on an SI engine, and although they initially saw promising results, the catalyst experienced 90% deactivation within 5 hours.[14] Thus, in order to successfully use H_2-rich reformate to extend the EGR limit and result in an overall engine efficiency benefit, the reforming process must be robust and impose a minimal fuel energy penalty. Ideally, the reforming process would achieve thermochemical recuperation (TCR), where waste heat in the exhaust is converted to usable chemical energy.

The concept of applying TCR in internal combustion engines to improve efficiency involves using exhaust heat to promote the catalytic reforming of hydrocarbon fuels to produce a mixture of hydrogen and carbon monoxide, typically referred to as syngas or reformate.[15,16] For TCR to occur, the enthalpy of the of the product reformate mixture must be higher than that of the initial reactants.[17,12] Numerous studies on the application of TCR in gas turbines for power plants have been published,[18–24] but the idea of using this method in internal combustion engines is more recent. Researchers examining the TCR approach have suggested benefits including increased work output of up to 13%[11,25] and improvements in engine efficiency ranging from 10-17%.[26–28] Additionally, the reforming potential of a wide variety of hydrocarbon fuels has been studied for both TCR and fuel cell applications. These include conventional fuels such as gasoline[12,29–31] and diesel,[16,32–34] along with alternative fuels such as ethanol,[17,27] methanol,[27,28] and natural gas.[35]

There are two approaches for reforming hydrocarbon fuels in internal combustion engines: steam reforming and partial oxidation reforming. The steam reforming reactions for iso-octane and

ethanol are shown in Reactions R1-R4 in Table 1, along with associated enthalpies of reaction on a per mole of fuel and per mole of C basis.[30,36,37] The ratio between the lower heating value (LHV) of the products and the LHV of the reactants is included as well. All four reactions have positive enthalpies of reaction and LHV_P/LHV_R ratios greater than one, illustrating that steam reforming is an endothermic process. This endothermic nature allows for a truly recuperative process, recycling exhaust energy in chemical form as reformate.[15,12] Unfortunately, achieving sufficient levels of hydrogen generation requires temperatures in excess of 600 °C,[15,19,36,38] which can be difficult to achieve and maintain in exhaust gas. Further, the endothermic reactions can decrease temperature sufficiently to shut down the reforming activity. Therefore, in order to make reforming more feasible for application to internal combustion engines, air can be added to provide oxygen for partial oxidation reforming.

The reactions which occur during partial oxidation reforming are shown in Reactions R5-R6 in Table 1.[39,40] These reactions are much more active at lower temperatures,[27,30] making this a suitable approach in a transient environment such as automotive exhaust. Unfortunately, partial oxidation reforming alone is exothermic, meaning a portion of fuel energy is lost as heat during reforming.[41,42] This reforming process is also less efficient at hydrogen production from a fuel usage standpoint, producing a much smaller number of moles of hydrogen per mole of fuel burned. However, in an environment where both oxygen and water vapor are present, both types of reforming can occur simultaneously.[35,43] Heat generated by the exothermic partial oxidation reactions can drive endothermic steam reforming.[44,45] Thus, the net energy balance of the total reforming process is highly dependent on the availability of both oxygen and heat in the system. Achieving optimal engine efficiency using this strategy requires a balance which achieves adequate hydrogen production without losing excessive energy as heat during reforming.

The current study assesses hydrocarbon fuel reforming over a Rh/Al_2O_3 reformer catalyst in simulated exhaust gas recirculation (EGR) loop conditions with three different fuels: iso-octane, ethanol, and gasoline. Performance durability and sulfur tolerance of the catalyst will be discussed in a subsequent publication.

2. Materials and methods

2.1 Catalyst

The reformer catalyst used in the current study is a pre-commercial formulation with 2 wt% Rh supported on Al_2O_3. Umicore synthesized the catalyst and coated it onto a zirconia-mullite substrate with a channel density of 400 cells per square inch. A 2 cm diameter by 2.5 cm long monolith core sample was cut from a full size substrate for use in the flow reactor experiments. The same core sample was used for all experiments reported here. The catalyst was not intentionally aged according to any specific protocol, but it was used for over 50 hours of partial oxidation and steam reforming experiments with methane and propane prior to the experiments discussed below.

2.2 Automated flow reactor

The activity of the Rh/Al_2O_3 reformer catalyst is measured using an automated flow reactor to simulate the conditions of an exhaust gas recirculation (EGR) loop. A diagram of this reactor is shown in Figure 1. MKS Instruments mass flow controllers meter the flow rates of gaseous species from compressed gas cylinders to achieve the desired gas mixture. Water vapor is introduced to the simulated exhaust mixture by a custom-designed vapor delivery system which uses an Eldex Laboratories HPLC pump to supply liquid water to a 1 m stainless steel tube with a 1.6 mm outer diameter (OD) wrapped in a coil around a 9.5 mm cartridge heater. After exiting

the stainless steel coil, the vaporized water is injected through a 100 mm stainless steel capillary with a 1.6 mm OD and 0.18 mm inner diameter (ID) into an inert gas stream of N_2 at 200 °C. A Chemyx syringe pump with a 250 mL stainless steel syringe injects liquid hydrocarbons (iso-octane, ethanol, and gasoline) through a separate stainless steel capillary with identical dimensions into the preheated gas stream. The flow reactor is comprised of stainless steel gas lines which have an OD of 6.4 mm and are heated to 200°C to prevent the condensation or adsorption of reacting gases.

A large cylindrical quartz tube with a 25 mm OD and 22 mm ID is used to house the Rh/Al_2O_3 catalyst core sample,. Alumina felt (1.5 mm thick) is wrapped tightly around the sample to ensure a snug fit and prevent gas bypass. This core sample is placed downstream of smaller quartz tubes (23 cm in length with a 3 mm OD and 1 mm ID) as shown in Figure 2. These smaller quartz tubes facilitate heat transfer to the simulated exhaust gases and create a more uniform inlet gas temperature at the catalyst face. The quartz tube reactor is placed into a Lindberg Blue M Mini Mite tubular furnace which provides control over the gas temperature. Custom-built stainless steel end caps located at each end of the large quartz tube are connected to the stainless steel gas lines of the flow reactor. Several ports are built into the stainless steel end caps to allow for thermocouples and pressure transducers. Three 0.5 mm diameter Omega Type K thermocouples provide temperature measurements at different locations: 5 mm upstream of the catalyst core inlet, at the catalyst core midpoint, and 5 mm downstream from the catalyst core outlet. The pressure at the inlet and exit of the quartz tube reactor is monitored using Omegadyne silicon diaphragm absolute pressure transducers. The flow reactor is controlled with a custom-designed LabVIEW interface which is used for data acquisition and allows the operator to program automated experimental protocols. An MKS Multigas 2030HS FTIR spectrometer and

Pfeiffer Vacuum Prisma-Plus QMG-220 mass spectrometer measures the simulated exhaust gas composition at both the inlet and outlet of the catalyst core and delivers this information to the LabVIEW interface. The mass spectrometer signals were calibrated by flowing known concentrations of the measured species (H_2, O_2, hydrocarbons) in the full simulated EGR mixture through a reactor bypass line at least once per day. All concentrations are reported on a wet basis (including water).

2.3 Experimental protocol

To simulate operation in the EGR loop of an engine operating with a stoichiometric air/fuel ratio, the reforming catalyst is continuously exposed to a flow of 700 sccm CO_2, 600 sccm H_2O, and 3700 sccm N_2, representing a synthetic exhaust mixture with a composition of 14% CO_2, 13% H_2O, and balance N_2. Varying flows of fuel and air are added to this base EGR mixture to investigate the performance of the reforming catalyst over a wide range of compositions. Reformer feed compositions are frequently described in terms of steam/carbon (S/C) and oxygen/carbon (O/C) ratios. For EGR loop applications, where the steam flow is essentially fixed at a given engine operating point, changing the S/C ratio corresponds to changing the fuel flow. Similarly, variations in O/C ratio are achieved by varying the air added to the base EGR mixture. The experiments conducted under the current study included a wide range of both S/C and O/C ratios in an effort to capture the behavior of the reforming catalyst across the relatively large operating space that could be observed under realistic EGR loop operation. In order to study fuel effects on reformer performance, three different fuels were evaluated: iso-octane, Decon Laboratoreis, Inc., 200 proof ethanol, and EEE Lube Certification Gasoline from Haltermann Solutions. The properties of the fuels investigated are provided in Table 2.

Steam reforming is examined by ramping the inlet gas temperature of the reformer catalyst from 400 to 800°C at 5°C/min and adding hydrocarbon fuel on a C_1 basis to achieve the desired S/C ratio. Ramps are performed for S/C ratios of 2.0, 1.5, and 1.0, which correspond to C_1 flow rates of 300 sccm, 400 sccm, and 600 sccm, respectively (details provided in Table 3). Partial oxidation experiments are conducted with fixed inlet gas temperatures of 400, 500, and 600 °C at S/C ratios of 1.0, 0.667, and 0.5. At each fixed temperature and S/C ratio a range of O/C ratios are evaluated by introducing O_2 and N_2 to simulate the addition of air. Prior to each O/C sweep, the catalyst is exposed to a mixture of simulated EGR and air for 15 min to clean any residual hydrocarbons or coke from the catalyst surface. Then the fuel flow is initiated and the O/C ratio is swept between 1.0 and either 0.1, 0.333, or 0.5, depending on S/C ratio. The flow composition at each individual O/C ratio during the sweep is held for fifteen minutes to ensure that steady state is achieved. Flow compositions during partial oxidation experiments for each fuel are shown in Tables 4-6. The minimum O/C ratio tested at each S/C point is calculated to maintain the S/C + O/C ratio at 1.0 or above to avoid coking, except in the case of ethanol where oxygen is present in the fuel. Complete oxidation of the fuel (to CO_2 and H_2O) is minimized by maintaining the O/C ratio below 1.0. The full array of experiments described above is performed for all three fuels included in the study.

3. Results and Discussion

3.1 Steam Reforming

Steam reforming is the ideal route for H_2 generation since it is a thermochemically recuperative process and produces a higher number of moles of H_2 per mole of fuel consumed relative to partial oxidation reforming (Table 1). The amount of H_2 produced by steam reforming with iso-

octane, ethanol, and gasoline is shown as a function of inlet gas temperature in Figures 3-5, respectively, along with the outlet temperature of the reformer catalyst. Iso-octane can generate up to 10% hydrogen over the catalyst, but the inlet gas temperature must be at least 700°C to produce concentrations of H_2 significant enough to improve the efficiency of the combustion process. Interestingly, increasing the fuel flow (thereby decreasing the S/C ratio) has a minimal effect on hydrogen generation. Normally, H_2 production would increase at higher fuel flows, as long as there is sufficient steam and heat to support the reforming process. Since there was more than enough steam to generate additional H_2 in our iso-octane study, it suggests that the steam reforming under these conditions is sensible enthalpy-limited. This is further demonstrated in Figure 3(b), which shows the catalyst outlet temperature as a function of inlet temperature. Since the steam reforming process is endothermic, conversion of the fuel to H_2 pulls heat out of the gas stream, decreasing the catalyst temperature. Eventually, the temperature of the gas gets so low that the kinetics of the steam reforming reaction become slow, and H_2 production shuts down. The H_2 production and catalyst temperature curves at the different fuel flow rates (H_2O/C ratios) overlay because the enthalpy available to drive the stem reforming reaction (in the form of sensible heat carried by the gas stream, as there is no external heat source) is the same for all three fuel flow rates. Once enough sensible enthalpy has been removed from the gas stream to drop the catalyst temperature below where it is active for steam reforming, H_2 production stops. In the case of ethanol fuel, shown in Figure 4, less hydrogen production is observed across the entire temperature range, but otherwise the trends are similar.

Measurements of steam reforming over the Rh/Al_2O_3 catalyst using gasoline resulted in drastically different hydrogen production curves relative to iso-octane and ethanol, which can be seen in Figure 5. The amount of hydrogen generated is much lower compared to both iso-octane

and ethanol, with a maximum concentration of 3% at 800 °C. Additionally, a decrease in hydrogen production was observed as the fuel added to the EGR mixture was increased. These phenomena can most likely be attributed to the presence of sulfur in the gasoline used in the current study. Sulfur has been shown to inhibit steam reforming Rh-based catalysts, and Ferrandon et al. found that sulfur tolerance can be improved by increasing the steam to carbon ratio, mirroring the trends observed for steam reforming with gasoline in the current study.[30,46]

Due to the sensible enthalpy-limited nature of steam reforming at these operating temperatures, as well as the sensitivity to even low levels of sulfur in the fuel, steam reforming does not appear to be a viable option for production of hydrogen over the Rh/Al_2O_3 catalyst in the EGR loop configuration.

3.2 Partial Oxidation Reforming

While catalytic steam reforming clearly faces challenges to implementation in engine applications, there are other methods to producing H_2 from hydrocarbon-based fuels. For example, catalytic partial oxidation, which involves mixing air with the fuel prior to sending it over a reforming catalyst, can produce significant quantities of H_2 at much lower temperatures than catalytic steam reforming because the heat required to keep the catalyst hot enough to drive the reforming process is generated by oxidation of a portion of the fuel feed. Since the EGR gas mixture to which the air and fuel is added contains a significant amount of water vapor, it is possible for the heat generated from fuel partial oxidation to drive the catalytic steam reforming, perhaps approaching a thermally neutral (also known as autothermal) or even net endothermic reaction. Obviously, for the complicated gas mixtures that would be encountered in an EGR loop reforming application, there is a wide range of chemical processes that could potentially occur

over the reforming catalyst. The dominant process(es) will depend strongly on the operating conditions, including the catalyst temperature, and the relative amounts of fuel, air, and steam fed to the catalyst. To capture as many different operating regimes as possible, the experiment matrix covered a wide range of conditions, and was repeated with the three different fuels: iso-octane, ethanol, and gasoline.

3.2.1 Iso-octane catalytic partial oxidation reforming

Iso-octane, a highly branched alkane, is representative of the fully saturated components of commercially-available gasoline, and is frequently used as a major component in surrogate gasoline mixtures.[47] Figure 6 shows the production of H_2 and reformate ($CO + H_2$) during catalytic reforming of iso-octane as a function of oxygen/carbon ratio (abscissa, controlled by air flow) at three catalyst inlet temperatures (data series, controlled by catalyst furnace) and three steam/carbon ratios (figure panels, determined by fuel flow). Figure 7 shows results from the same experiments, but plots H_2 and reformate production as a fraction of fuel enthalpy fed to the catalyst. This replotting of the data allows visualization of the reforming energy balance, which is further aided by the addition of a third set of lines showing the total recovery of fuel enthalpy at the catalyst outlet. It should be noted that the fractional enthalpy plots are based on the enthalpy content of the major products at the outlet of the reforming catalyst, including H_2, CO, CH_4, and unconverted iso-octane. The calculated catalyst outlet enthalpies did not include the contributions of less abundant reforming products, such as cracked or partially oxidized fuel species (such as aldehydes or alkenes). For the case of iso-octane, ignoring these less abundant species does not appear to have a significant impact on the overall thermodynamic analysis. However, for more reactive or more complicated fuel mixtures, such product species could significantly impact the net energy balance (see subsequent discussion on other fuels).

From a high-level perspective, catalytic partial oxidation reforming of iso-octane is a very effective method for generating H_2 for an internal combustion engine. Under optimal operating conditions, the effluent from the reforming catalyst contains nearly 15% H_2 and upwards of 10% CO (Figure 6). These concentrations should be more than sufficient to provide significant benefits to engine operation. The effects of the key operating parameters (temperature, oxygen to carbon ratio, steam to carbon ratio) on both H_2 production and reforming energy balance for iso-octane are discussed in more detail below.

3.2.1.1 Iso-octane reforming: effect of catalyst temperature

Each panel of Figure 6 contains two sets of curves, one for H_2 and one for reformate. There are three curves in each set, one for each inlet temperature that was included in the reforming experiments. These inlet temperatures (nominally 400, 500, and 600 °C) cover the approximate range of exhaust temperatures expected in an EGR loop for a stoichiometric gasoline engine under normal driving conditions. Looking at Figure 6(a), increasing the catalyst inlet temperature increases the amount of reformate produced. This trend is expected, as increasing the catalyst temperature will increase the rate of the reforming reactions, thereby increasing the quantity of reforming products. The increased catalytic activity at higher temperatures is also apparent in Figure 7(a): at 600 °C and high O/C ratios, essentially all of the enthalpy in the catalyst effluent is reformate, meaning none of the iso-octane remains unconverted. Figure 7(a) also illustrates the beneficial effect of higher temperatures on the reforming energy balance: higher temperatures result in higher enthalpy retained in the catalyst effluent. In fact, at some of the 600 °C operating points, the amount of enthalpy in the effluent is actually higher than the fuel enthalpy fed to the catalyst. The increase in enthalpy indicates that some of the reformate is formed through steam

reforming. Figure 3 showed that this catalyst is at least somewhat active for steam reforming of iso-octane at 600 °C.

3.2.1.2 Iso-octane reforming: effect of oxygen/carbon ratio

The abscissa for all of the plots in Figures 6 and 7 is the molar oxygen/carbon (O/C) ratio. Note that this ratio includes O atoms in the form of O_2 fed to the catalyst as air, not the O atoms present in the H_2O included to simulate the EGR mixture. Also, as mentioned in the experimental section, $H_2O/C + O/C$ was never allowed to drop below 1.0 to reduce the potential for coking of the catalyst. Thus, at higher fuel feed rates, the lower O/C points were not run (Table 3).

Catalytic partial oxidation reforming conditions are often described in terms of O/C, as this is a convenient way to capture the relative amounts of air and fuel fed to the reforming catalyst. An O/C ratio of 1.0 would be a stoichiometric mixture for converting all of the fuel to CO and H_2 (see, for example, reaction R5). Since the intent for this particular study is to integrate the reforming catalyst with an internal combustion engine, a secondary axis for the fuel/air equivalence ratio (ϕ) is also shown Figures 6 and 7. The equivalence ratio is defined such that $\phi = 1$ is a stoichiometric mixture for complete combustion of the fuel to CO_2 and H_2O. A mixture with $\phi < 1$ is fuel-lean (excess air), while a mixture with $\phi > 1$ is fuel-rich (excess fuel). For the experiments reported here, O/C is controlled by changing the amount of air added to the simulated EGR at a fixed fuel flow. Increasing O/C ratio corresponds to increasing air flow. As can be seen in Figures 6 and 7, for O/C of 1.0, ϕ is roughly 3, which is a very rich mixture from a combustion perspective. As the O/C ratio decreases, ϕ increases exponentially.

As expected, O/C ratio has a strong impact on both H_2 production (Figure 6) and overall reforming energy balance (Figure 7). When no air is fed to the catalyst, the O/C ratio is 0, which corresponds to the steam reforming conditions discussed in section 3.1, where minimal reformate is generated at low catalyst inlet temperatures. However, once air is added to the feed stream, some of the fuel reacts with O_2 over the reforming catalyst, generating heat and increasing the catalyst temperature. Higher temperatures increase the catalytic activity, producing more reformate and increasing fuel conversion. This trend is most apparent at an inlet gas temperature of 400 °C in Figures 6(a) and 7(a): as the O/C ratio is increased, the catalyst gets hotter, and both fuel conversion and reformate production increase. The effect of increasing O/C on reformate production is a bit more complicated for the higher inlet temperature cases. At 600 °C (Figure 6(a)), reformate production increases from O/C 0.1 up to 0.7, but then it decreases with further addition of air. As discussed previously, there is some steam reforming activity at the higher inlet catalyst temperatures. Since some of the fuel is reacting with water vapor, less O_2 is required to convert all of the remaining fuel. Under these conditions, if extra air is added, it begins to over-oxidize the fuel, or oxidize the reformate, generating CO_2 and H_2O instead of the desired CO and H_2 products. This reduces the reformate production at higher inlet temperatures and O/C ratios. High O/C ratios also reduce the total enthalpy content of the catalyst effluent (Figure 7(a)) at all temperatures. Again, this occurs because a larger fraction of the fuel fed to the catalyst is being converted to fully oxidized products (CO_2 and H_2O) rather than reformate.

The balance between catalytic steam reforming and catalytic partial oxidation of the fuel can be more easily visualized by looking at how the gas temperature changes across the catalyst. As an example case, Figure 8 shows the temperature at the inlet, midpoint, and exit of the reformer catalyst for all three S/C ratios for the experiments performed at 500°C. The largest difference

occurs between the inlet and midpoint of the catalyst, suggesting this is the area of most interest. This is in agreement with observations by Carrera et al., who found that, during catalytic partial oxidation experiments with iso-octane over a Rh/Al_2O_3 catalyst, a hot spot tends to form near the catalyst inlet before the formation of water and subsequent steam reforming processes lowered the catalyst temperature further downstream moving towards the catalyst exit.[45] Comparing the midpoint and outlet temperatures for all three cases in Figure 8, the temperature decreases by roughly the same amount regardless of O/C ratio and reformate yields. A similar drop in temperature between the midpoint and outlet is observed in the absence of fuel feed (indicated by horizontal dashed lines in Figure 8). Thus, the temperature drop in the back half of the catalyst is due to heat loss to the ambient rather than chemical processes inside the catalyst. Therefore, the subsequent discussions regarding temperature will focus on the front half of the catalyst, where Carrera et al. showed the bulk of the chemical reactions occur. [45]

Figure 9 shows the change in temperature from the inlet to the midpoint of the catalyst ($T_{cat,mid} - T_{cat,in}$), for all of the experimental points included in Figures 6 and 7. A positive change in temperature indicates the temperature is increasing in the front half of the catalyst, which can only be due to an exothermic process occurring inside the catalyst (note that the catalyst was placed outside the heated zone of the furnace, so there are no external heat sources that could cause this temperature increase). Conversely, a negative change in temperature means that heat is being removed from the gas stream through endothermic reactions, heat losses to the ambient, or both. For an inlet temperature of 400 °C in Figure 9(a), the catalyst shows a small increase in temperature low O/C ratios, and the midpoint temperature steadily increases with increasing O/C ratio. The inlet temperature is too low to support steam reforming. As more air is added to the feed gas, an increasing fraction of the fuel is oxidized, generating more heat and increasing the

catalyst temperature. Some of this heat drives endothermic steam reforming, but some is lost to heating the gas temperature high enough for steam reforming activity. Thus, the steady increase in catalyst midpoint temperature with increasing O/C is consistent with both higher reformate production (Figure 6) and lower fuel enthalpy retention (Figure 7). The temperature difference trends are quite different for an inlet temperature of 600 °C. At low O/C ratios, the temperature drop across the front half of the catalyst is essentially the same as that measured in the absence of fuel (the horizontal dashed lines). Here, the inlet temperature is already high enough for steam reforming, so less of the heat generated by oxidation of the fuel is used to increase the temperature of the incoming gas stream and more is available to drive the endothermic steam reforming reaction. The nearly autothermal reforming process at 600 °C results in higher retention of the fuel enthalpy in the catalyst effluent (Figure 7). As more air is added, the temperature drop across the front half of the catalyst stays relatively constant up to an O/C of about 0.7, and the fraction of fuel enthalpy retained in the catalyst effluent remains high even as reformate production increases significantly. Above an O/C of 0.7, the catalyst midpoint temperature increases more rapidly as additional air is added. This more rapid rise in catalyst midpoint temperature is consistent with the drop in reformate concentration and fuel enthalpy retention in Figures 6 and 7. Since the catalyst is active for steam reforming at this temperature, some of the iso-octane reacts with H_2O rather than O_2. As a result, less O_2 is required to convert all of the iso-octane to reformate. Based on the trends in midpoint temperature, reformate concentration, and enthalpy retention for a catalyst inlet temperature of 600 °C, it appears that O/C ratios greater than 0.7 result in complete oxidation of some of the iso-octane to CO_2 and H_2O, resulting in a larger exotherm over the catalyst and reduced reformate production. The 500

°C case falls between the 400 °C and 600 °C data sets, spanning the range form thermally neutral at low O/C to exothermic at high O/C.

The reduction of total enthalpy retained in the catalyst effluent at high O/C ratios has an interesting consequence regarding the selection of optimal operating strategies for EGR loop reforming: inlet conditions that generate the highest H_2 concentrations will not necessarily be the most thermodynamically beneficial. The overall reforming energy balance is actually best at lower O/C ratios, where less fuel enthalpy is lost to complete oxidation of the fuel. However, these conditions generate significantly lower concentrations of H_2.

The key question that still needs to be answered is whether the lower concentrations of H_2 generated under the more energetically favorable reforming conditions will be sufficient to extend the EGR dilution limit and enable an overall boost in engine system efficiency. Thus, full evaluations of the overall thermodynamic benefit of the EGR loop reforming process will require integrating the reforming catalyst with an engine to capture both the enthalpy losses over the catalyst as well as the engine efficiency benefits enabled by reformate.

The interplay between catalyst inlet temperature and O/C ratio will also need to be considered when selecting and evaluating operating strategies for the reforming catalyst since the optimal amount of air to add to the EGR and fuel mixture will depend on the catalyst temperature. Higher air feeds (up to O/C of 1.0) are more beneficial for reformate production at lower temperatures. However, at higher inlet temperatures, the optimal O/C ratio for reformate production is significantly lower.

3.2.1.3 Iso-octane reforming: effect of H_2O/C ratio

Since the experiments described here were designed to mimic operation in the EGR loop of a stoichiometric engine, the H_2O concentration in the baseline gas mixture was held fixed for all of the experiments. The only way to change the H_2O/C ratio under such operating constraints is by changing fuel feed. Thus, some of the trends discussed below may be counterintuitive to those who work on more traditional reforming applications, where H_2O/C ratio is typically controlled by changing the H_2O feed while holding the fuel feed constant. In these experiments, decreasing H_2O/C corresponds to increasing fuel feed.

The effects of decreasing H_2O/C can be seen by looking at the panels from top to bottom (a to c) in Figures 6, 7, and 9. Perhaps the most obvious conclusion to draw from these plots is that changing H_2O/C has minimal effect on the overall trends discussed above for catalyst inlet temperature and O/C. Aside from the smaller data sets at lower H_2O/C ratios (to avoid the potential for catalyst coking), the overall reforming energetics shown in Figure 7 are very similar across all three H_2O/C ratios. The primary effect of decreasing H_2O/C by adding more fuel to the EGR mixture is to generate higher concentrations of reformate, as shown in Figure 6. In fact, the most promising reformer performance is obtained at the highest fuel feed rate (lowest H_2O/C) and highest inlet temperature (600 °C), where an O/C ratio of 0.5 generates roughly 12% H_2 while still retaining all of the fuel enthalpy. These results make catalytic partial oxidation look like a promising approach to onboard H_2 generation, at least for iso-octane.

3.2.2 Ethanol catalytic partial oxidation reforming

Ethanol, a primary alcohol, is blended to a level of 10-15 % by volume in nearly all of the gasoline sold in the U.S. Given its prevalence in gasoline, and the potential for it to have very

different reforming activity relative to hydrocarbons, ethanol was a logical choice for inclusion in this study.

3.2.2.1 Ethanol reforming: reformate production

The production of H_2 and reformate as a function of O/C ratio, inlet temperature, and H_2O/C during catalytic partial oxidation reforming of ethanol is shown in Figure 10. Overall, these plots look very similar to those for iso-octane in Figure 6. Ethanol produces similar quantities of reformate and slightly higher concentrations of H_2. Increasing catalyst temperature leads to higher reformate production due to higher catalyst activity. As O/C ratio is increased, reformate production initially increases, but then drops off at higher O/C ratios as increasing air flow begins to convert some of the ethanol to CO_2 and H_2O. Perhaps the biggest difference between iso-octane and ethanol is that the peak in reformate production occurs at a lower O/C ratio for ethanol than it did for iso-octane at all inlet temperatures evaluated. This is due to the O content of ethanol: as shown in reaction R7, an O/C of 0.5 is stoichiometric for complete conversion of ethanol to CO and H_2. If the O/C ratios are higher than 0.5 there is a potential to over-oxidize the fuel, resulting in a drop in the reformate production. Finally, decreasing H_2O/C (by increasing fuel flow) results in higher reformate production at all temperatures and O/C ratios, as with iso-octane.

3.2.2.2 Ethanol reforming: energy balance

While reformate production with ethanol predominately mirrors the behavior observed with iso-octane, the recovery of fuel enthalpy during ethanol reforming is much different compared to iso-octane, as shown in Figures 11(a)-11(c). At O/C ratios below 0.4, the fraction of fuel enthalpy retained is actually highest at 400°C, followed by 500°C and then 600°C. This is

especially noticeable at the highest S/C ratio of 1.0, where fuel enthalpy recovery never reaches 100% with an inlet gas temperature of 600°C. Additionally, unlike iso-octane where enthalpy retained in the catalyst effluent steadily declines as more air is added to the mixture, the enthalpy retention during ethanol reforming declines at low O/C ratios, before trending upwards again in the O/C range of 0.4-0.8, depending on temperature. This phenomenon can be attributed, at least in part, to the partial oxidation of ethanol to acetaldehyde, shown in Reaction R7.

$$CH_3CH_2OH + 0.5O_2 \rightarrow CH_3CHO + H_2O \qquad \Delta H_R^{\Theta} = \text{-178.5 KJ/mol} \qquad \text{(R7)}$$

Partial oxidation to acetaldehyde is an exothermic process, resulting in lower enthalpy retention in the catalyst effluent. The conversion of ethanol to acetaldehyde is shown in Figures 11(a)-12(c). Figure 12 shows that a significant fraction of the ethanol fed to the catalyst (upwards of 30% under some conditions) is converted to acetaldehyde. Comparing Figures 12 and 11, the peak in acetaldehyde formation as function of O/C ratio roughly corresponds to the minima in enthalpy retention in the at mid-level O/C ratios. It should also be noted that the partial oxidation of ethanol can produce additional species aside from acetaldehyde. These species are difficult to measure accurately with FTIR, and thus the total energy balance could be affected. At higher O/C ratios, the concentration of acetaldehyde diminishes for all three evaluation temperatures, but the fraction of fuel enthalpy retained in the catalyst effluent continues to decrease in a manner similar to that seen with iso-octane as the excess air flow generates more H_2O and CO_2.

3.2.2.3 Ethanol reforming: catalyst temperature

The change in temperature across the front half of the catalyst during catalytic partial oxidation reforming of ethanol is shown in Figure 13. As with iso-octane, the reforming process is net exothermic when the catalyst inlet temperature is 400 °C, which is too low for steam reforming.

However, at 600 °C inlet temperature, the reforming process results in a drop in the temperature across the front half catalyst larger than that observed with no fuel flow at all O/C ratios, likely due to endothermic steam reforming. Unlike iso-octane, which showed a continuous increase in midpoint temperature with increasing air feed, ethanol reforming results in a much more complicated relationship between catalyst midpoint temperature and O/C ratio. At low O/C ratios and lower inlet temperatures, the catalyst midpoint temperature increases with increasing air feed. This is likely due to the partial oxidation of ethanol to acetaldehyde, which is exothermic (see reaction 7). At the mid-level O/C ratios, this trend reverses, and catalyst midpoint temperature decreases with increasing O/C. This reversal in the midpoint temperature trend occurs at the same O/C ratios where acetaldehyde formation starts to drop off and reformate production peaks, consistent with the theory that the exothermic nature of the reforming process at low O/C ratios is driven, at least in part, by acetaldehyde formation. At the highest O/C ratios, the temperature trend reverses yet again, and higher air feeds result in increasing midpoint temperature due to complete oxidation of some of the ethanol to CO_2 and H_2O, which is exothermic.

Overall, catalytic partial oxidation of ethanol generates levels of reformate comparable to that of iso-octane. However, the formation of byproducts such as acetaldehyde makes the thermodynamics of the reforming process less favorable, and may cause issues with combustion control or materials compatibility when fed to an engine.

3.2.3 Gasoline catalytic partial oxidation reforming

The third fuel evaluated for EGR loop reforming feasibility is a certification gasoline. Obviously, this fuel is the most relevant for real world vehicle application. The gasoline is a fully formulated

refinery product with a composition similar to that found in pump gasoline, with two notable exceptions: it does not contain any ethanol, and the sulfur concentration (4 ppm by weight) is somewhat low.

3.2.3.1 Gasoline reforming: reformate production

Hydrogen and reformate generation for the certification gasoline are shown in Figures 14(a)-14(c). The production of H_2 and total reformate from the gasoline is significantly lower than for the other fuels. Where iso-octane and ethanol generated H_2 concentrations of 15% or more under optimal conditions, the gasoline only produces about 10% H_2. At lower fuel feeds, the drop is even more significant: the gasoline only produces about half as much H_2 as iso-octane. Aside from the reduction in total output, the trends in H_2 and reformate production with the various operating parameters evaluated for this study look very similar to those for iso-octane: increasing temperature increases catalyst activity, generating more H_2; reformate production increases with air feed up to the highest O/C ratios tested, at which point it starts to drop off due to production of CO_2 and H_2O; and decreasing H_2O/C (by increasing fuel feed) increases reformate production for all temperatures and O/C ratios.

As with the poor hydrogen production observed during steam reforming of the gasoline, it is likely that sulfur is inhibiting the performance of the Rh/Al_2O_3 catalyst by adsorbing to the catalyst surface.[29,46] Cracknell et al. suggest that sulfur causes an initial deactivation before plateauing, resulting in performance below that which would be expected of sulfur-free fuel.[48] Separate experiments (not reported here) that included exposure to SO_2 resulted in reversible deactivation of the catalyst, reducing reformate yield and fuel enthalpy retention while SO_2 was fed to the catalyst. Thus, while the Rh/Al_2O_3 catalyst is capable of stable hydrogen and syngas

production from a sulfur-containing gasoline, its performance remains consistently lower than observed with both ethanol and iso-octane, which do not contain any sulfur.

3.2.3.2 Gasoline reforming: energy balance

The fraction of fuel enthalpy retained in the catalyst effluent during catalytic partial oxidation reforming of gasoline is shown in Figures 15(a)-15(c). Gasoline reforming is thermodynamically more expensive than reforming of either iso-octane or ethanol, as demonstrated by the much lower retention of total fuel enthalpy from the catalyst effluent. In fact, there are very few operating points that come close to retaining all of the fuel enthalpy in the catalyst effluent. However, there are three factors which must be considered when examining fuel enthalpy retention for gasoline. First, the gasoline contains a significant fraction of aromatics, which tend to be more reactive in reforming than the alkane components, as shown in Figures 16(a)-16(c). Due to the lower hydrogen content per mole of carbon contained in these species, less potential for reforming to hydrogen exists. Partial oxidation reforming of aromatics is more exothermic than alkanes, reducing the enthalpy retention in the catalyst effluent.

Second, speciation is complicated with gasoline due to the numerous components which make up the fuel. Measuring all of these components accurately is extremely challenging using the FTIR and mass spectrometer, meaning the energy balance may be missing components which could increase the overall amount of recapture measured. This is especially problematic at lower O/C ratios, where the fuel conversion is low and thus the number of constituents is greatest. Therefore, although the energetics of gasoline reforming do not appear promising, they may be somewhat better than shown in Figure 15.

Finally, as discussed in the prior section, the sulfur content of the gasoline likely poisons active sites critical for steam reforming, which reduces endothermic reforming and adversely impacts the overall energy balance for catalytic partial oxidation reforming.

3.2.3.2 Gasoline reforming: catalyst temperature

The temperature change in the front half of the catalyst during gasoline reforming, shown in Figure 17, is quite different from what was observed with the other fuels. The shape of the curves is somewhat similar to those seen for iso-octane. However, where iso-octane reforming was exothermic at low inlet temperatures and thermally neutral at high inlet temperatures, gasoline reforming is exothermic across nearly the entire operating envelope. The more exothermic nature of the reforming process is consistent with the reduced H_2 production and less favorable energy balance, all of which can be explained by lower steam reforming activity due to sulfur poisoning of the catalyst.

4. Conclusions

The potential for generating hydrogen and reformate using a Rh/Al_2O_3 catalyst located within an engine EGR loop was investigated for iso-octane, ethanol, and gasoline. The studies were performed on a simulated exhaust flow reactor over a range of inlet gas temperature and simulated exhaust gas conditions. It was determined that steam only reforming, with no oxygen included in the simulated exhaust gas feed, is not a viable route for hydrogen generation due to the high temperature required to reach syngas concentrations required for engine efficiency benefits. Gasoline, in particular, shows extremely poor performance during steam reforming, which may be due to the presence of sulfur in the fuel inhibiting catalyst activity.

Partial oxidation reforming with water vapor present in the simulated exhaust feed is much more promising, generating concentrations of hydrogen in the range of 10-16% under peak conditions. However, there is a tradeoff between maximum hydrogen production and the recovery of the original fuel enthalpy, as the air flows required to generate high catalyst temperatures and reformate yields also lead to more complete oxidation of the fuel to CO_2 and H_2O, converting some of the fuel energy to heat.. Of the three fuels studied here, iso-octane exhibits the best overall performance, while ethanol is comparable but is less favorable from an energy balance standpoint due to the partial oxidation of ethanol to acetaldehyde. As with steam reforming, gasoline produces the lowest concentrations of hydrogen, and determining the energy balance is challenging as a result of the difficulty in identifying and measuring the numerous species contained within gasoline accurately.

Overall, it was found that partial oxidation reforming of liquid fuels in a simulated EGR mixture over the Rh/Al_2O_3 catalyst demonstrated sufficiently high reformate yields and favorable energetics to warrant further evaluation in the EGR system of a stoichiometric combustion engine.[49,50] The net impact of EGR loop reforming on engine efficiency will depend on EGR gas temperature and composition as well as fuel properties. Future studies will investigate the durability of this process.

Acknowledgements

This research was supported by the U.S. Department of Energy, Office of Energy Efficiency and Renewable Energy, Vehicle Technologies Office. The authors gratefully acknowledge the support and guidance of program managers Gurpreet Singh and Michael Weismiller at DOE. The authors also gratefully acknowledge John Nunan of Umicore for providing catalyst samples and Galen Fisher of the University of Michigan for supporting our efforts to obtain substrates and catalysts.

Disclaimer

This manuscript has been authored by UT-Battelle, LLC, under Contract No. DEAC0500OR22725 with the U.S. Department of Energy. The United States Government retains and the publisher, by accepting the article for publication, acknowledges that the United States Government retains a non-exclusive, paid-up, irrevocable, world-wide license to publish or reproduce the published form of this manuscript, or allow others to do so, for United States Government purposes. DOE will provide public access to these results of federally sponsored research in accordance with the DOE Public Access Plan (http://energy.gov/downloads/ doe-public-access-plan).

(1) Splitter, D.; Pawlowski, A.; Wagner, R. *Front. Mech. Eng.* **2016**, *1* (16).

(2) Caton, J. A. *SAE Tech.* **2013**, 2013-01–0266.

(3) Alger, T.; Mangold, B.; Roberts, C.; Gingrich, J. *SAE Int. J. Engines* **2012**, *5* (3), 2012-01–1149.

(4) Kaul, B. C.; Finney, C. E. A.; Wagner, R. M.; Edwards, M. L. *SAE Int. J. Engines* **2014**, *7* (2), 2014-01–1236.

(5) Cairns, A.; Blaxill, H.; Irlam, G. *SAE Tech. Pap.* **2006**, 2006-01–0047.

(6) Duchaussoy, Y.; Lefebvre, A.; Bonetto, R. *SAE Tech. Pap.* **2003**, 2003-01–0629.

(7) Martz, J. B.; Middleton, R. J.; Lavoie, G. A.; Babajimopoulos, A.; Assanis, D. N. *Combust. Flame* **2011**, *158* (6), 1089–1096.

(8) Stone, C. R.; Brown, A. G.; Beckwith, P. *SAE Tech. Pap.* **1996**, 960613.

(9) Szybist, J. P.; Splitter, D. *SAE Int. J. Engines* **2016**, *9* (2), 2016-01–0715.

(10) Alger, T.; Gingrich, J.; Mangold, B. *SAE Tech. Pap. 2007-01-0475* **2007**, 2001-01–0475.

(11) Ivanič, Ž.; Ayala, F.; Goldwitz, J.; Heywood, J. B. *SAE Int. Tech. Pap.* **2005**, No. 724.

(12) Fennell, D.; Herreros, J.; Tsolakis, A.; Xu, H.; Cockle, K.; Millington, P. *SAE Tech. Pap. Ser.* **2013**, 2013-01–0537.

(13) Hwang, J.; Li, X.; Northrop, W. *SAE Int.* **2017**, 2017-01–0757.

(14) Ashida, K.; Maeda, H.; Araki, T.; Hoshino, M.; Hiraya, K.; Izumi, T.; Yasuoka, M. *SAE*

Int. J. Fuels Lubr. **2015**, *8* (2), 2015-01–0902.

(15) Chakravarthy, V. K.; Daw, C. S.; Pihl, J. A.; Conklin, J. C. *Energy and Fuels* **2010**, *24* (3), 1529–1537.

(16) Kang, I.; Bae, J. *J. Power Sources* **2006**, *159* (2), 1283–1290.

(17) Tartakovsky, L.; Baibikov, V.; Gutman, M.; Mosyak, A.; Veinblat, M. *SAE Tech. Pap. Ser.* **2011**, 2011-01–1992.

(18) Basu, A.; Rajagopal, S. *United Stats Pat.* **2001**, Patent No. US 6,223,519 B1.

(19) Verkhivker, G.; Kravchenko, V. *Energy* **2004**, *29* (3), 379–388.

(20) Harvey, S. P.; Knoche, K. F.; Richter, H. J. *Gas Turbines* **1995**, *24* (117).

(21) Alves, L. G.; Nebra, S. A. *Energy* **2004**, *29* (12–15 SPEC. ISS.), 2385–2395.

(22) Carapellucci, R. *Energy Convers. Manag.* **2009**, *50* (5), 1218–1226.

(23) Huber, D. J.; Bannister, R. L.; Khinkis, M. J.; Rabovitser, J. K. *United Stats Pat.* **1997**, Patent No. 5,595,059.

(24) Carapellucci, R.; Milazzo, A. *Energy Convers. Manag.* **2005**, *46* (18–19), 2936–2953.

(25) Kweon, C.-B.; Khinkis, M. J.; Nosach, V. G.; Zabransky, R. F. *United Stats Pat.* **2008**, Patent No. US 2005/0279333 A1.

(26) Posada, F.; Bedick, C.; Clark, N. N.; Kozlov, A.; Linck, M.; Boulanov, D.; Pratapas, J. *SAE Tech. Pap.* **2007**, 2007-01–4074.

(27) Tartakovsky, L.; Baibikov, V.; Veinblat, M. *SAE/KSAE 2013 Int. Powertrains, Fuels Lubr. Meet. FFL 2013, Oct. 21, 2013 - Oct. 23* **2013**, *11*.

(28) Poran, A.; Artoul, M.; Sheintuch, M.; Tartakovsky, L. M. *SAE Int. J. Engines* **2014**, *7* (1), 234–242.

(29) Hoshino, M.; Izumi, T.; Akama, H.; Zaima, M.; Hiraya, K.; Ashida, K.; Araki, T.; Maeda, H. *SAE Tech. Pap. Ser.* **2015**, 2015-01–1955.

(30) Qi, A.; Wang, S.; Ni, C.; Wu, D. *Int. J. Hydrogen Energy* **2007**, *32* (8), 981–991.

(31) Ashur, M.; Misztal, J.; Wyszynski, M. L.; Tsolakis, A.; Xu, H. M.; Qiao, J.; Golunski, S. *SAE Tech. Pap.* **2007**, 2007-24–0078.

(32) Sitshebo, S.; Tsolakis, A.; Elghawi, U.; Theinnoi, K.; Wyszynski, M. L.; Cracknell, R. F.; Clark, R. H. *SAE Pap.* **2009**, No. 2009-01–0276.

(33) Kaila, R. K.; Krause, A. O. I. *Int. J. Hydrogen Energy* **2006**, *31* (13), 1934–1941.

(34) Welaya, Y. M. A.; El Gohary, M. M.; Ammar, N. R. *Alexandria Eng. J.* **2012**, *51* (2), 69–75.

(35) He, Z.; Xu, Z.; Zhu, L.; Zhang, W.; Fang, J.; Lin, H.; Guan, B.; Huang, Z.; Hu, J.; Chu, L. *SAE Int.* **2016**, 2016-01–2239.

(36) Vaidya, P. D.; Rodrigues, A. E. *Chem. Eng. J.* **2006**, *117* (1), 39–49.

(37) Ni, M.; Leung, D. Y. C.; Leung, M. K. H. *Int. J. Hydrogen Energy* **2007**, *32* (15 SPEC. ISS.), 3238–3247.

(38) Rostrup-Nielsen, J. R. *Catal. Today* **2009**, *145* (1–2), 72–75.

(39) Kaltschmitt, T.; Diehm, C.; Deutschmann, O. *Ind. Eng. Chem. Res.* **2012**, *51* (22), 7536–7546.

(40) de Lima, S. M.; da Cruz, I. O.; Jacobs, G.; Davis, B. H.; Mattos, L. V.; Noronha, F. B. *J. Catal.* **2008**, *257* (2), 356–368.

(41) Cai, W.; Wang, F.; Zhan, E.; Van Veen, A. C.; Mirodatos, C.; Shen, W. *J. Catal.* **2008**, *257* (1), 96–107.

(42) Kirwan, J. E.; Quader, A. A.; Grieve, M. J. *SAE Tech. Pap.* **1999**, 1999-01–2927.

(43) Benito, M.; Sanz, J. L.; Isabel, R.; Padilla, R.; Arjona, R.; Daza, L. *J. Power Sources* **2005**, *151* (1–2), 11–17.

(44) Carrera, A.; Pelucchi, M.; Stagni, A.; Beretta, A.; Groppi, G. *Int. J. Hydrogen Energy* **2017**, *42* (39), 24675–24688.

(45) Carrera, A.; Beretta, A.; Groppi, G. *Ind. Eng. Chem. Res.* **2017**, *56* (17), 4911–4919.

(46) Ferrandon, M.; Mawdsley, J.; Krause, T. *Appl. Catal. A Gen.* **2008**, *342* (1–2), 69–77.

(47) Morgan, N.; Smallbone, A.; Bhave, A.; Kraft, M.; Cracknell, R.; Kalghatgi, G. *Combust. Flame* **2010**, *157* (6), 1122–1131.

(48) Cracknell, R. F.; Kramer, G. J.; Vos, E. *Sae Pap. 2004-01-1926* **2004**, 2004-01–1926.

(49) Chang, Y.; Szybist, J. P.; Pihl, J. A.; Brookshear, D. W. *Submitted for Publication Consideration to Energy and Fuels, December 2017.*.

(50) Chang, Y.; Szybist, J. P.; Pihl, J. A.; Brookshear, D. W. *Submitted for Publication Consideration to Energy and Fuels, December 2017*.

(51) Anderson, J. E.; Dicicco, D. M.; Ginder, J. M.; Kramer, U.; Leone, T. G.; Raney-Pablo, H. E.; Wallington, T. J. *Fuel* **2012**, *97*, 585–594.

Table 1. Steam reforming and partial oxidation reforming reactions for iso-octane and ethanol.

Steam Reforming Reactions	ΔH_R^{Θ} (KJ/mol)	ΔH_R^{Θ}/mol C (KJ/mol C)	LHV_P/LHV_R	
$C_8H_{18} + 8H_2O \rightarrow 17H_2 + 8CO$	+945.2	+159.3	1.25	(R1)
$C_8H_{18} + 16H_2O \rightarrow 25H_2 + 8CO_2$	+1274.5	+118.2	1.19	(R2)
$CH_3CH_2OH + H_2O \rightarrow 4H_2 + 2CO$	+254.8	+63.7	1.20	(R3)
$CH_3CH_2OH + 3H_2O \rightarrow 6H_2 + 2CO_2$	+172.5	+43.1	1.14	(R4)
Partial Oxidation Reforming Reactions	ΔH_R^{Θ} (KJ/mol)	ΔH_R^{Θ}/mol C (KJ/mol C)	LHV_P/LHV_R	
$C_8H_{18} + 4O_2 \rightarrow 9H_2 + 8CO$	-660.1	-82.5	0.87	(R5)
$CH_3CH_2OH + 0.5O_2 \rightarrow 3H_2 + 2CO$	+12.94	+3.2	1.01	(R6)

Table 2. Properties of EEE Lube Certification Gasoline

Fuel Property	Iso-Octane	Ethanol	Gasoline
Saturates (vol%)	100	0	71.2
Aromatics (vol%)	0	0	27.8
Olefins (vol%)	0	0	1.1
Ethanol (vol%)	0	100	0
C (wt%)	84.1	52.1	86.5
H (wt%)	15.9	13.1	13.3
O (wt%)	0	34.7	<0.01
S (wt%)	0	0	7
RON (-)	100	109	97.0
MON (-)	100	90[51]	88.7

Table 3. Flow conditions during steam reforming with iso-octane, ethanol, and gasoline.

Iso-octane

H_2O/C	GHSV (h^{-1})	N_2	CO_2	H_2O	C_8H_{18}
2	38500	73.4%	13.9%	11.9%	0.7%
1.5	38600	73.3%	13.9%	11.9%	1.0%
1	38800	72.9%	13.8%	11.8%	1.5%

Ethanol

H_2O/C	GHSV (h^{-1})	N_2	CO_2	H_2O	CH_3CH_2OH
2	39100	71.8%	13.7%	11.7%	2.9%
1.5	39300	71.2%	13.6%	11.7%	3.8%
1	39700	69.8%	13.5%	11.5%	5.7%

Gasoline

H_2O/C	GHSV (h^{-1})	N_2	CO_2	H_2O	C_1
2	40500	69.8%	13.2%	11.3%	5.7%
1.5	41300	68.5%	13.0%	11.1%	7.4%
1	42800	66.1%	12.5%	10.7%	10.7%

Table 4. Flow conditions during partial oxidation reforming with iso-octane.

H_2O/C	O/C	GHSV (h^{-1})	N_2	CO_2	H_2O	O_2	C_8H_{18}
1	1	49700	74.3%	10.8%	9.2%	4.6%	1.2%
1	0.9	48600	74.1%	11.0%	9.4%	4.2%	1.2%
1	0.8	47500	74.0%	11.3%	9.6%	3.9%	1.2%
1	0.7	46400	73.9%	11.5%	9.9%	3.5%	1.2%
1	0.6	45300	73.8%	11.8%	10.1%	3.0%	1.3%
1	0.5	44200	73.7%	12.1%	10.4%	2.6%	1.3%
1	0.4	43100	73.5%	12.4%	10.6%	2.1%	1.3%
1	0.3	42100	73.4%	12.7%	10.9%	1.6%	1.4%
1	0.2	41000	73.2%	13.1%	11.2%	1.1%	1.4%
1	0.1	39900	73.1%	13.4%	11.5%	0.6%	1.4%
0.667	1	55500	74.3%	9.6%	8.3%	6.2%	1.5%
0.667	0.9	53800	74.2%	9.9%	8.5%	5.7%	1.6%
0.667	0.8	52200	74.0%	10.2%	8.8%	5.3%	1.6%
0.667	0.7	50500	73.9%	10.6%	9.1%	4.8%	1.7%
0.667	0.6	48900	73.7%	10.9%	9.4%	4.2%	1.8%
0.667	0.5	47300	73.5%	11.3%	9.7%	3.6%	1.8%
0.667	0.4	45600	73.3%	11.7%	10.0%	3.0%	1.9%
0.667	0.333	44500	73.2%	12.0%	10.3%	2.6%	1.9%
0.5	1	61200	74.4%	8.7%	7.5%	7.5%	1.9%
0.5	0.9	59000	74.2%	9.1%	7.8%	7.0%	1.9%
0.5	0.8	56800	74.1%	9.4%	8.1%	6.5%	2.0%
0.5	0.7	54600	73.9%	9.8%	8.4%	5.9%	2.1%
0.5	0.6	52500	73.6%	10.2%	8.7%	5.2%	2.2%
0.5	0.5	50300	73.4%	10.6%	9.1%	4.6%	2.3%

Table 5. Flow conditions during partial oxidation reforming with ethanol.

H_2O/C	O/C	GHSV (h^{-1})	N_2	CO_2	H_2O	O_2	CH_3CH_2OH
1	1	51400	71.8%	10.4%	8.9%	4.5%	4.5%
1	0.9	50300	71.6%	10.6%	9.1%	4.1%	4.6%
1	0.8	49200	71.4%	10.9%	9.3%	3.7%	4.7%
1	0.7	48100	71.3%	11.1%	9.5%	3.3%	4.8%
1	0.6	47000	71.1%	11.4%	9.7%	2.9%	4.9%
1	0.5	46000	70.9%	11.6%	10.0%	2.5%	5.0%
1	0.4	44900	70.7%	11.9%	10.2%	2.0%	5.1%
1	0.3	43800	70.5%	12.2%	10.5%	1.6%	5.2%
1	0.2	42700	70.3%	12.5%	10.7%	1.1%	5.4%
1	0.1	41600	70.1%	12.9%	11.0%	0.6%	5.5%
0.667	1	58000	71.0%	9.2%	7.9%	5.9%	5.9%
0.667	0.9	56400	70.8%	9.5%	8.1%	5.5%	6.1%
0.667	0.8	54800	70.6%	9.8%	8.4%	5.0%	6.3%
0.667	0.7	53100	70.3%	10.1%	8.6%	4.5%	6.5%
0.667	0.6	51500	70.0%	10.4%	8.9%	4.0%	6.7%
0.667	0.5	49800	69.7%	10.7%	9.2%	3.4%	6.9%
0.667	0.4	48200	69.4%	11.1%	9.5%	2.9%	7.1%
0.667	0.3	46600	69.1%	11.5%	9.8%	2.2%	7.4%
0.667	0.2	44900	68.7%	11.9%	10.2%	1.5%	7.7%
0.667	0.1	43300	68.3%	12.4%	10.6%	0.8%	7.9%
0.5	1	64600	70.5%	8.3%	7.1%	7.1%	7.1%
0.5	0.9	62500	70.2%	8.6%	7.3%	6.6%	7.3%
0.5	0.8	60300	69.8%	8.9%	7.6%	6.1%	7.6%
0.5	0.7	58100	69.5%	9.2%	7.9%	5.5%	7.9%
0.5	0.6	55900	69.1%	9.6%	8.2%	4.9%	8.2%
0.5	0.5	53700	68.7%	10.0%	8.5%	4.3%	8.5%
0.5	0.4	51500	68.3%	10.4%	8.9%	3.6%	8.9%
0.5	0.3	49300	67.8%	10.8%	9.3%	2.8%	9.3%
0.5	0.2	47200	67.3%	11.3%	9.7%	1.9%	9.7%
0.5	0.1	45000	66.7%	11.9%	10.2%	1.0%	10.2%

Table 6. Flow conditions during partial oxidation reforming with gasoline.

H_2O/C	O/C	GHSV (h^{-1})	N_2	CO_2	H_2O	O_2	C_1
1	1	53700	68.7%	10.0%	8.5%	4.3%	8.5%
1	0.9	52600	68.5%	10.2%	8.7%	3.9%	8.7%
1	0.8	51500	68.3%	10.4%	8.9%	3.6%	8.9%
1	0.7	50400	68.0%	10.6%	9.1%	3.2%	9.1%
1	0.6	49300	67.8%	10.8%	9.3%	2.8%	9.3%
1	0.5	48200	67.5%	11.1%	9.5%	2.4%	9.5%
1	0.4	47200	67.3%	11.3%	9.7%	1.9%	9.7%
1	0.3	46100	67.0%	11.6%	10.0%	1.5%	10.0%
1	0.2	45000	66.7%	11.9%	10.2%	1.0%	10.2%
1	0.1	43900	66.4%	12.2%	10.4%	0.5%	10.4%
0.667	1	61500	67.1%	8.7%	7.5%	5.6%	11.2%
0.667	0.9	59800	66.7%	8.9%	7.7%	5.2%	11.5%
0.667	0.8	58200	66.4%	9.2%	7.9%	4.7%	11.8%
0.667	0.7	56600	66.0%	9.5%	8.1%	4.3%	12.2%
0.667	0.6	54900	65.6%	9.7%	8.3%	3.8%	12.5%
0.667	0.5	53300	65.2%	10.0%	8.6%	3.2%	12.9%
0.667	0.4	51600	64.8%	10.4%	8.9%	2.7%	13.3%
0.667	0.333	50500	64.5%	10.6%	9.1%	2.3%	13.6%
0.5	1	69200	65.8%	7.7%	6.6%	6.6%	13.2%
0.5	0.9	67000	65.4%	8.0%	6.8%	6.2%	13.7%
0.5	0.8	64900	64.9%	8.2%	7.1%	5.7%	14.1%
0.5	0.7	62700	64.4%	8.5%	7.3%	5.1%	14.6%
0.5	0.6	60500	63.9%	8.8%	7.6%	4.5%	15.2%
0.5	0.5	58300	63.3%	9.2%	7.9%	3.9%	15.7%

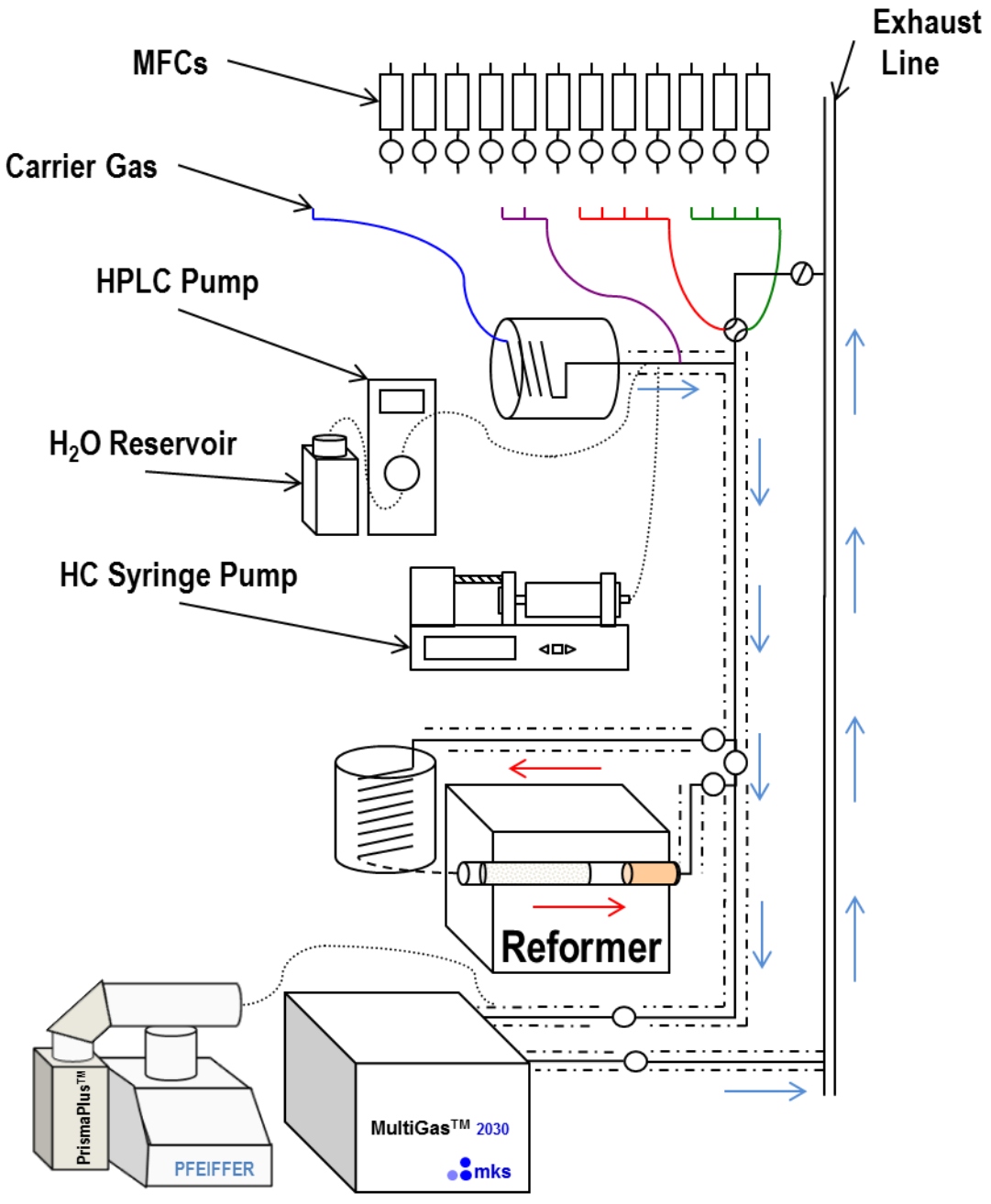

Figure 1. Diagram of automated flow reactor used to simulate EGR exhaust gas for reformer

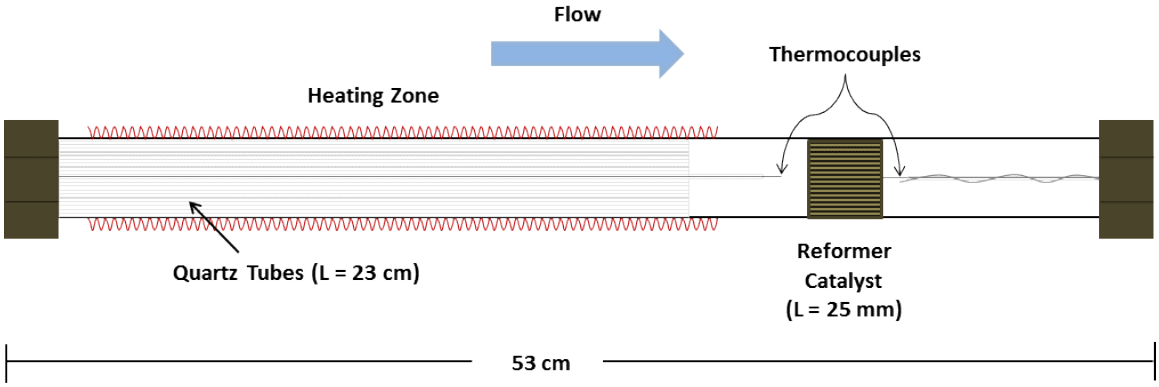

Figure 2. Quartz tube reactor setup on automated flow reactor.

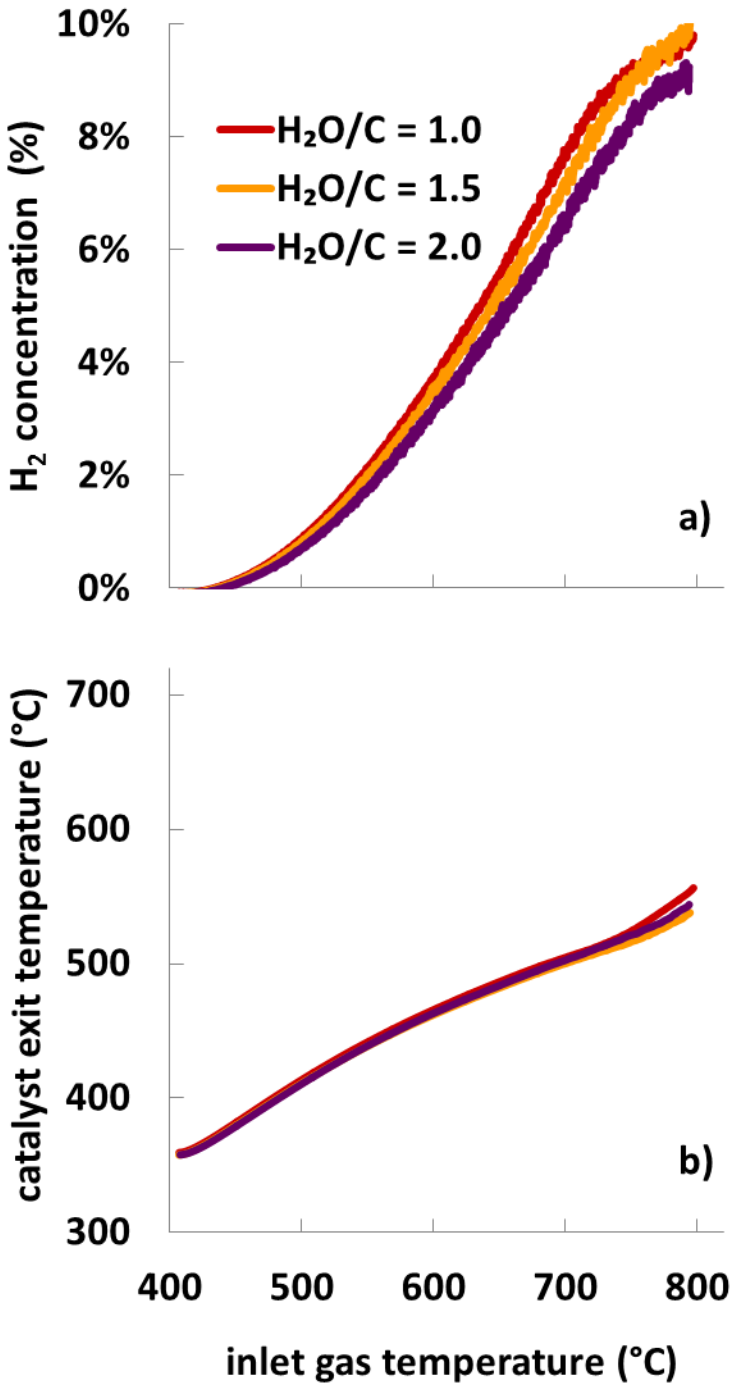

Figure 3. Measurements of a) hydrogen concentration and b) catalyst outlet temperature during steam reforming ramps with iso-octane at H_2O/C ratios of 1.0, 1.5, and 2.0.

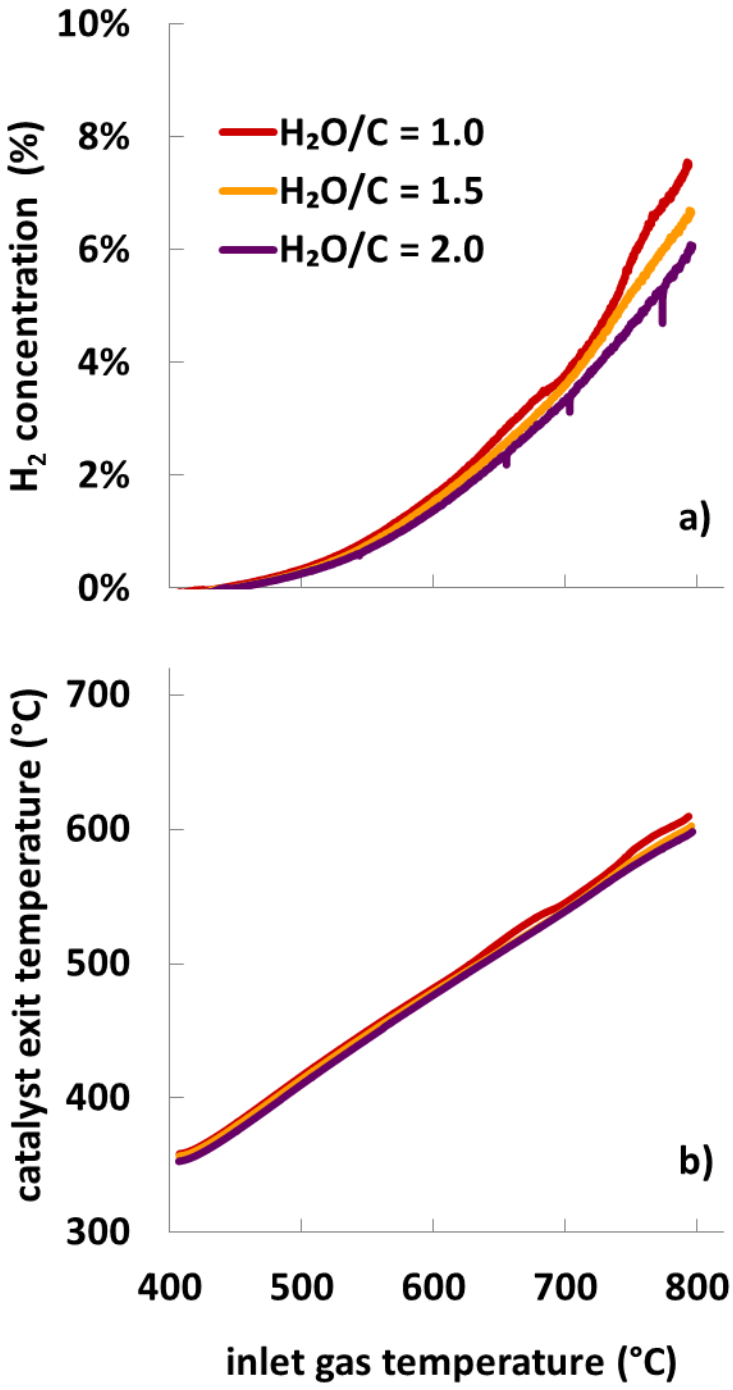

Figure 4. Measurements of a) hydrogen concentration and b) catalyst outlet temperature during steam reforming ramps with ethanol at H_2O/C ratios of 1.0, 1.5, and 2.0.

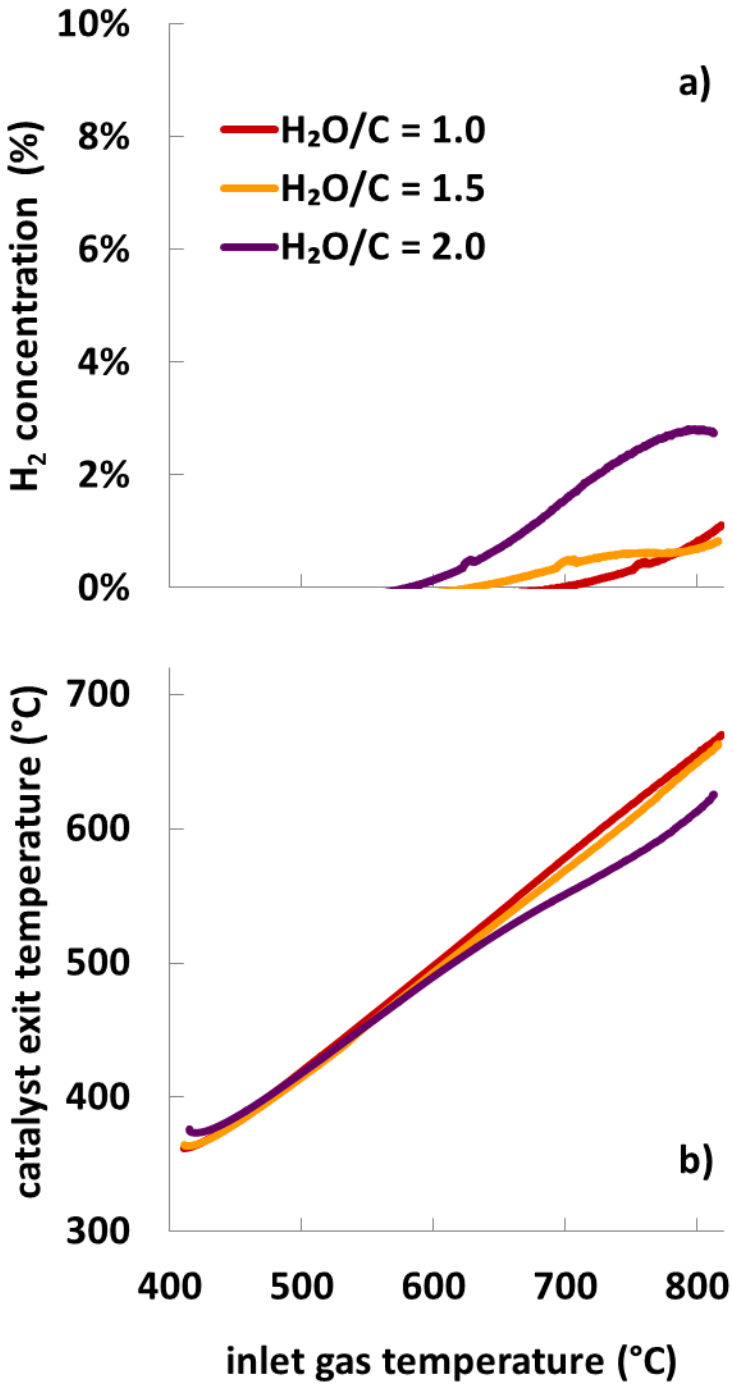

Figure 5. Measurements of a) hydrogen concentration and b) catalyst outlet temperature during steam reforming ramps with gasoline at H_2O/C ratios of 1.0, 1.5, and 2.0.

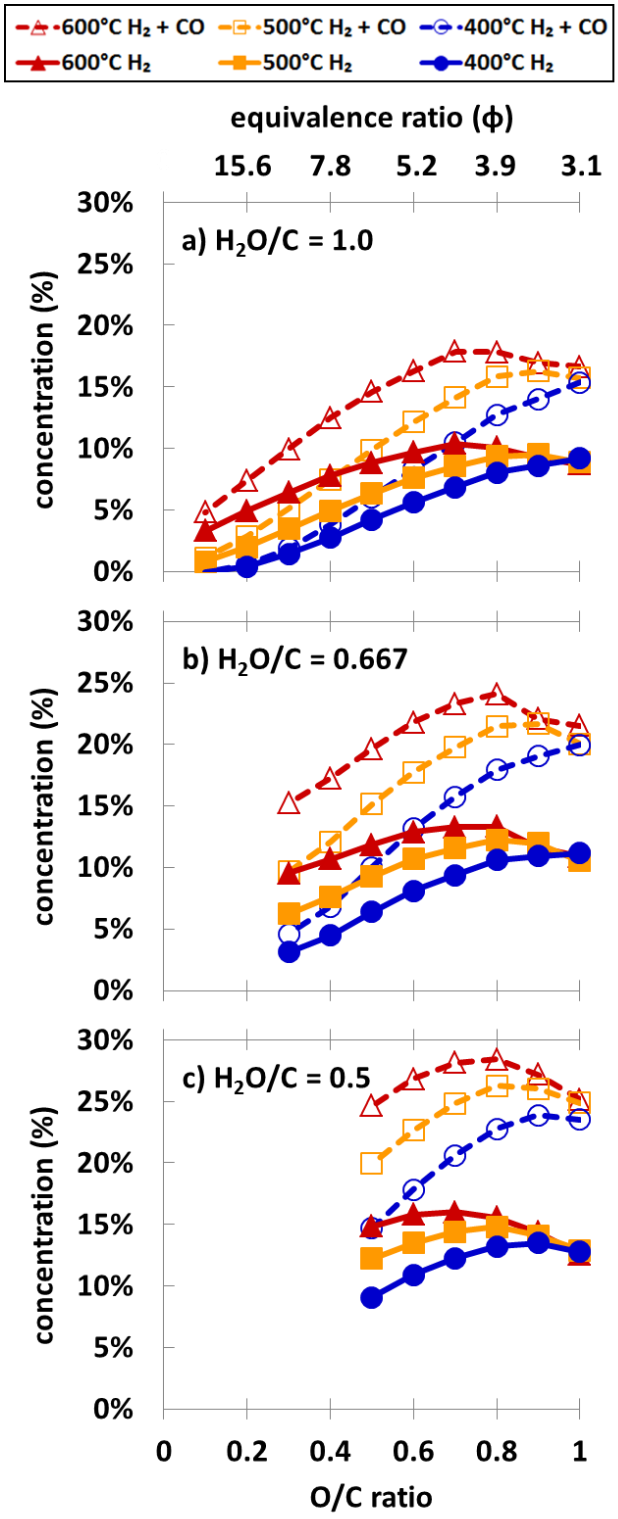

Figure 6. Hydrogen and reformate production during partial oxidation reforming of iso-octane in the presence of water vapor at S/C ratios of a) 1.0, b) 0.667, and c) 0.5.

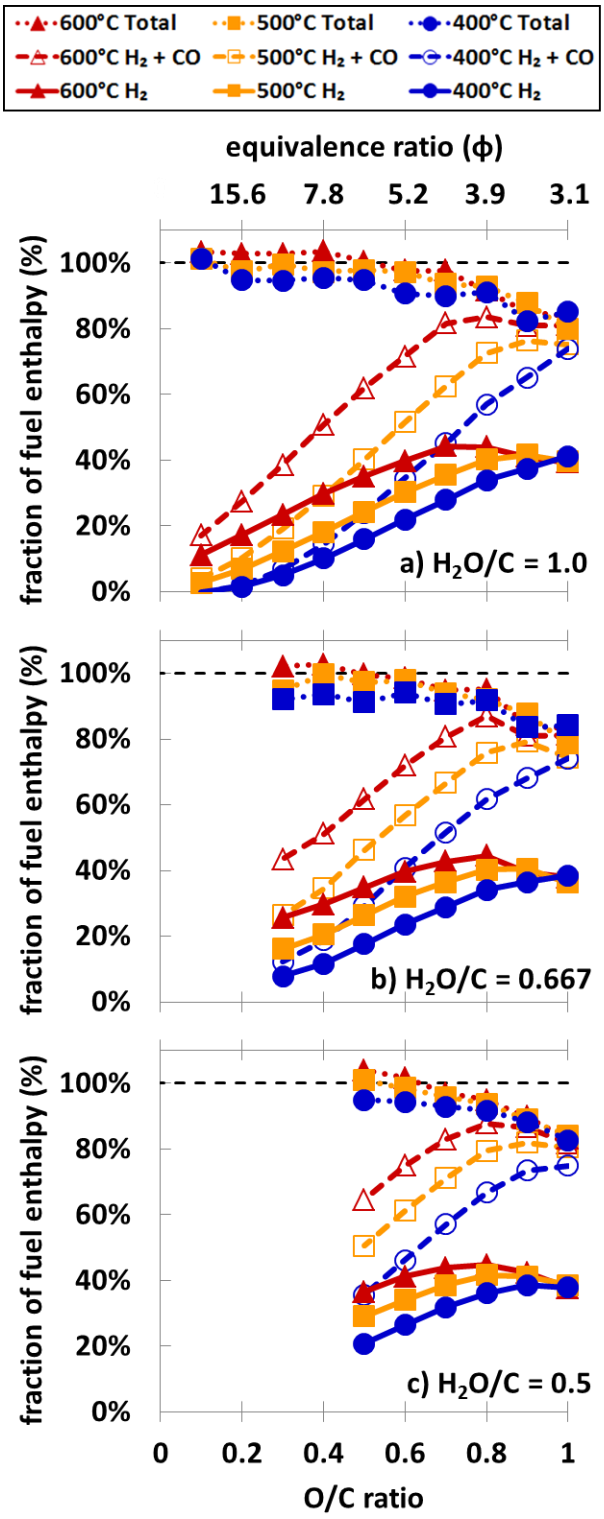

Figure 7. Fraction of fuel enthalpy recaptured during partial oxidation reforming of iso-octane in the presence of water vapor at S/C ratios of a) 1.0, b) 0.667, and c) 0.5.

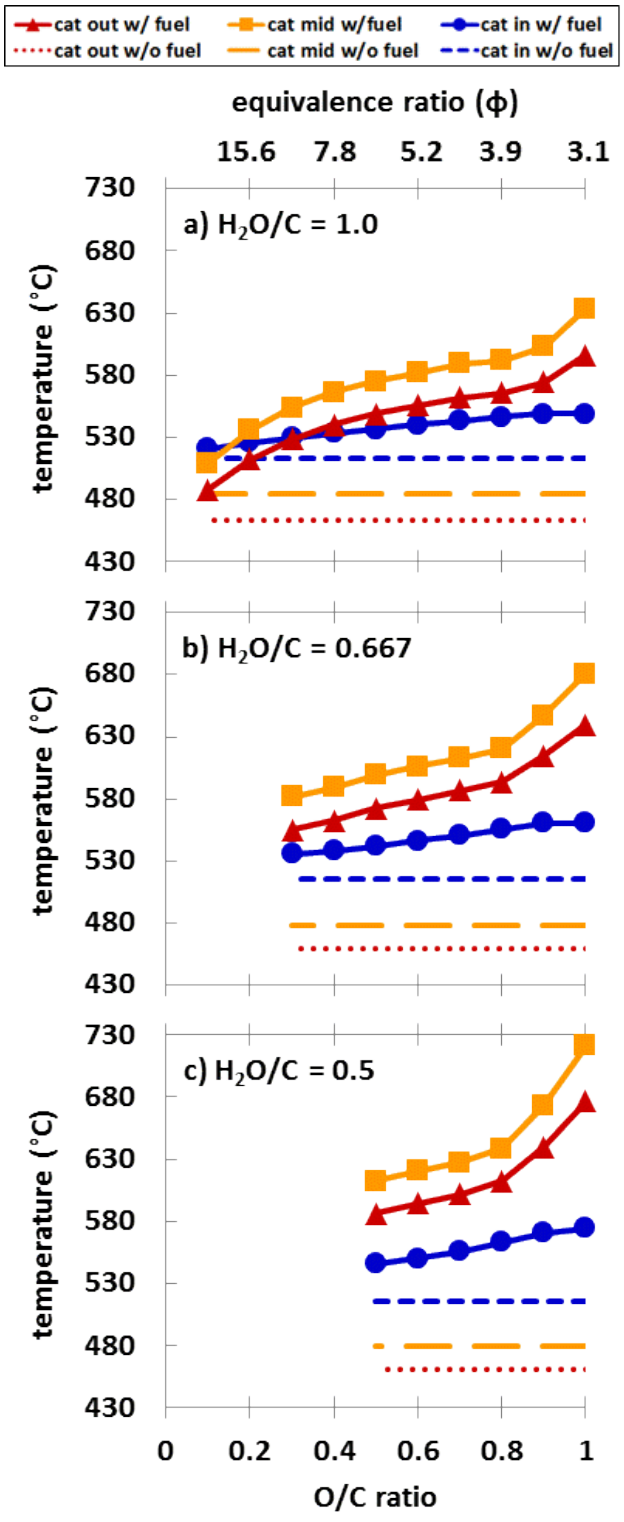

Figure 8. Temperatures at the catalyst inlet, midpoint, and outlet during partial oxidation reforming of iso-octane in the presence of water vapor at S/C ratios of a) 1.0, b) 0.667, and c) 0.5.

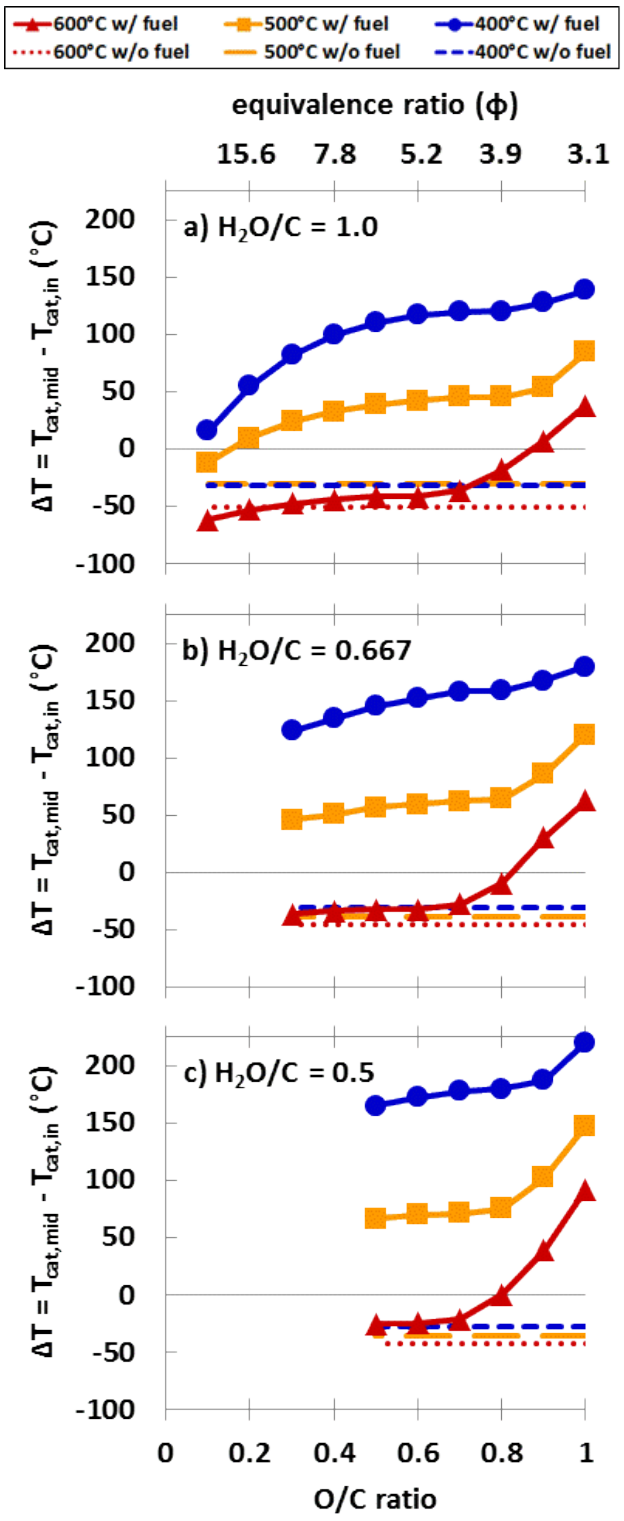

Figure 9. Temperature change from inlet to midpoint of catalyst during partial oxidation reforming of iso-octane in the presence of water vapor at S/C ratios of a) 1.0, b) 0.667, and c) 0.5.

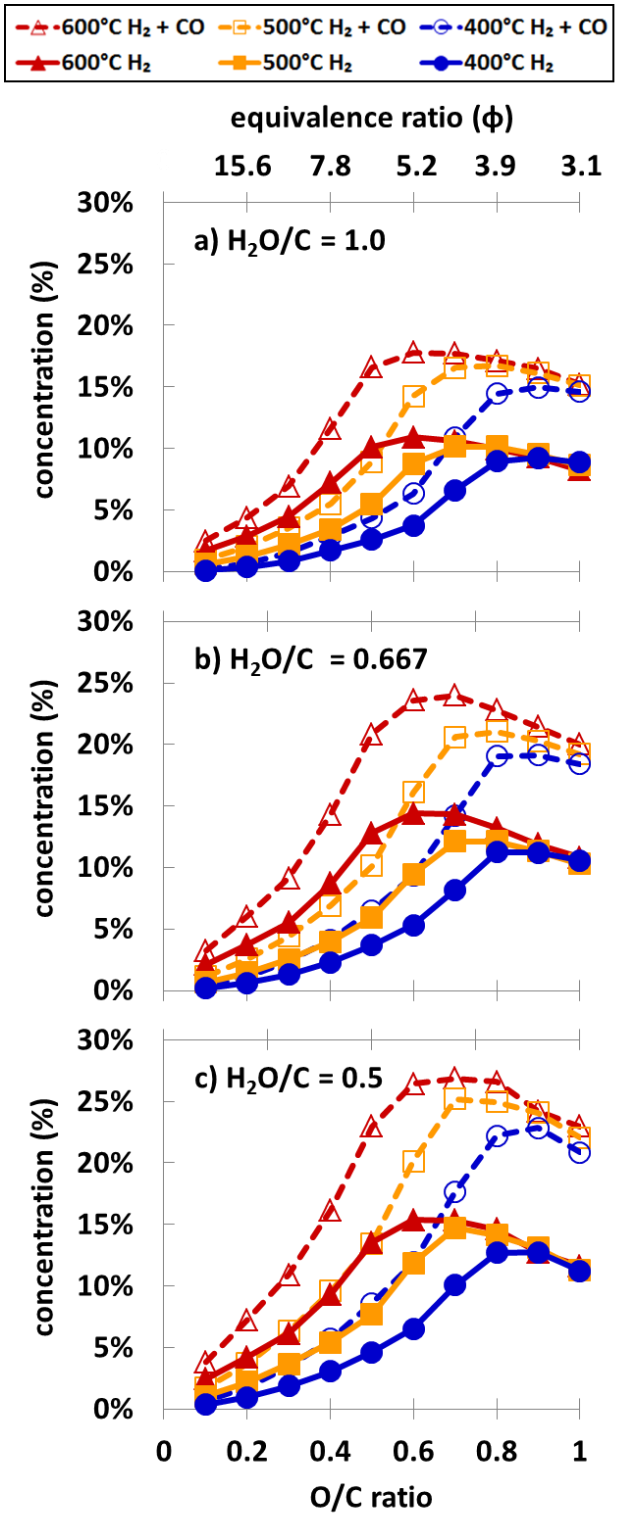

Figure 10. Hydrogen and reformate production during partial oxidation reforming of ethanol in the presence of water vapor at S/C ratios of a) 1.0, b) 0.667, and c) 0.5.

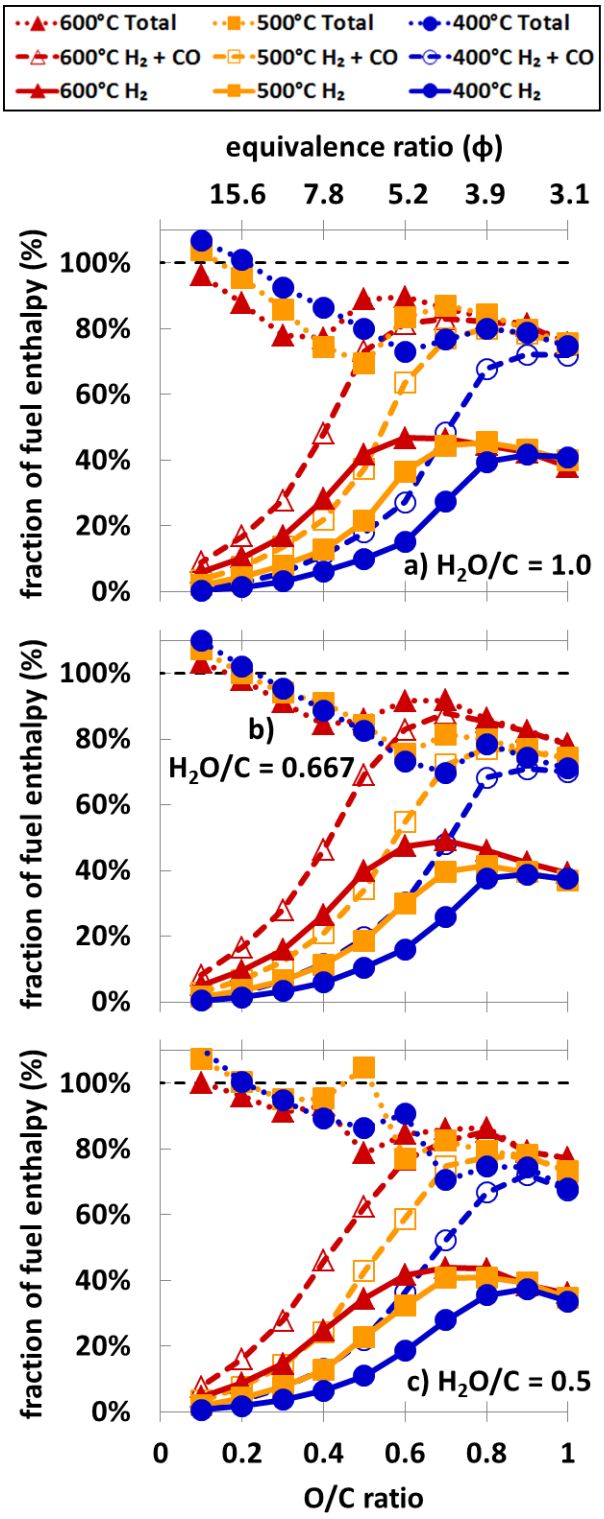

Figure 11. Fraction of fuel enthalpy recaptured during partial oxidation reforming of ethanol in the presence of water vapor at S/C ratios of a) 1.0, b) 0.667, and c) 0.5.

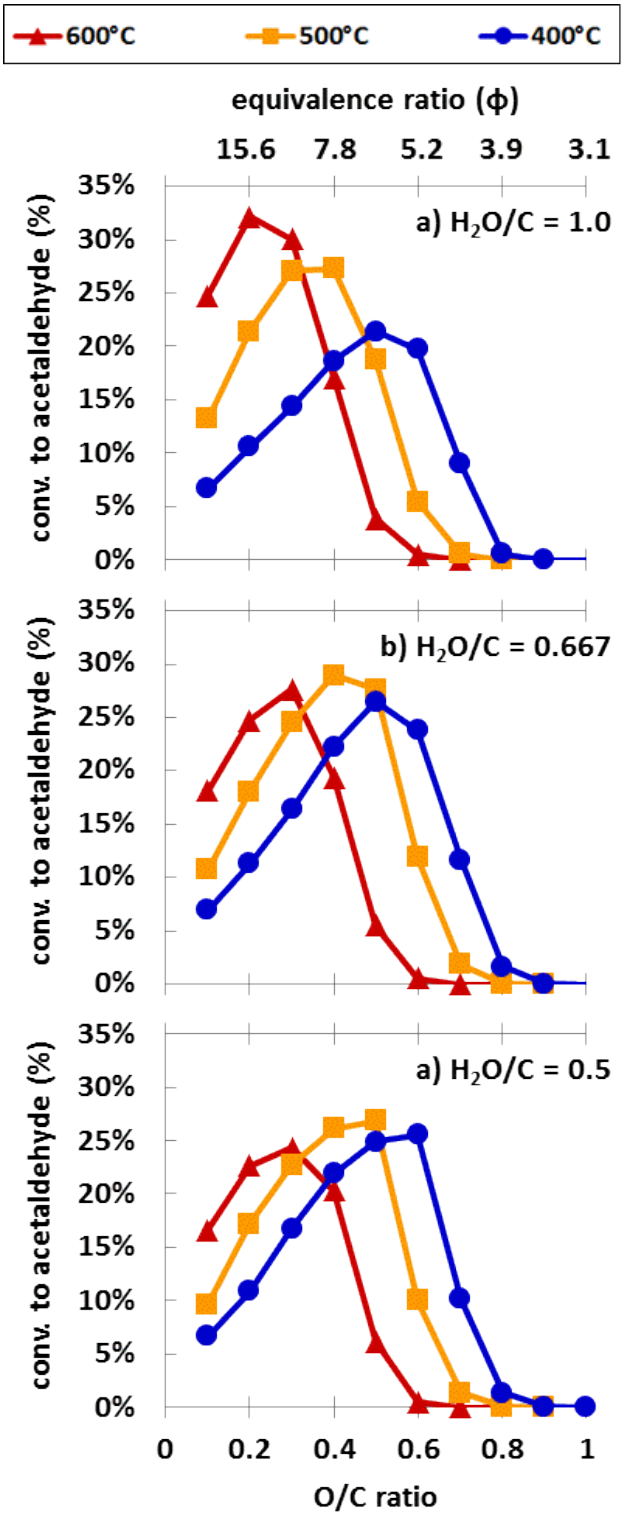

Figure 12. Conversion of ethanol to acetaldehyde during partial oxidation reforming of ethanol in the presence of water vapor at S/C ratios of a) 1.0, b) 0.667, and c) 0.5.

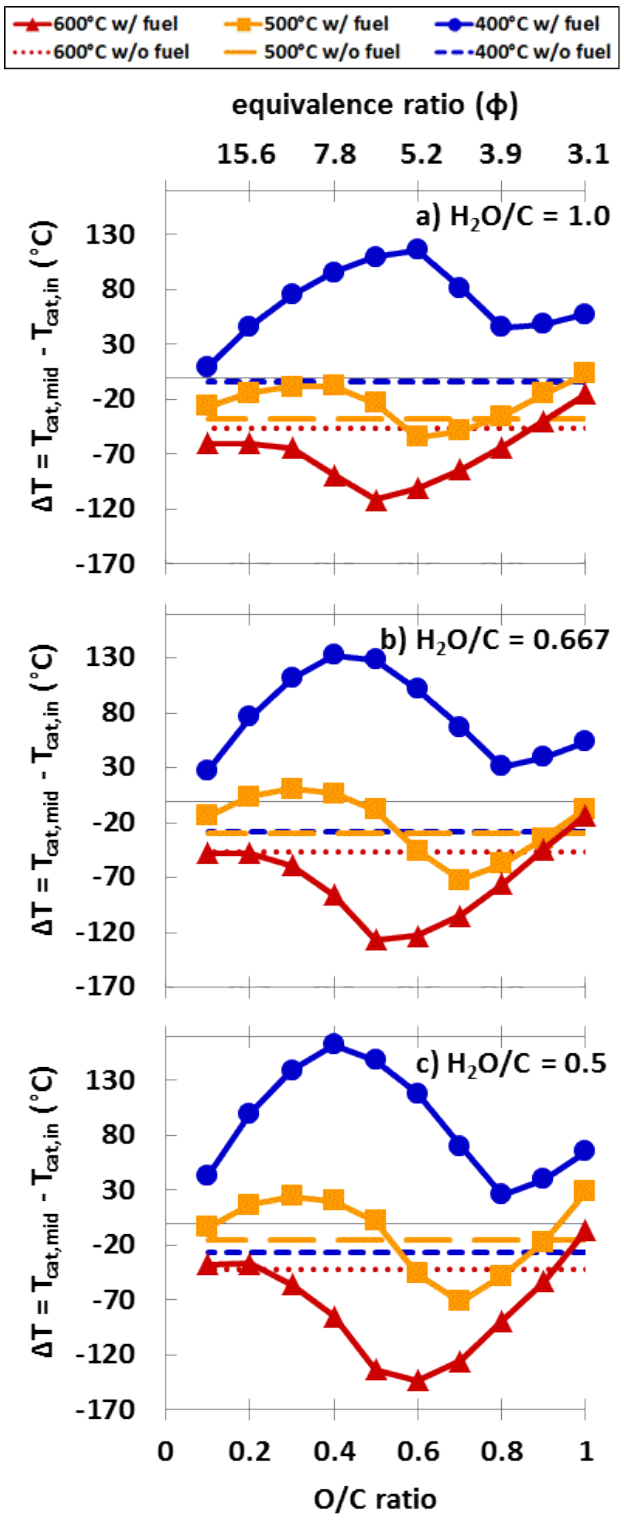

Figure 13. Temperature change from inlet to midpoint of catalyst during partial oxidation reforming of ethanol in the presence of water vapor at S/C ratios of a) 1.0, b) 0.667, and c) 0.5.

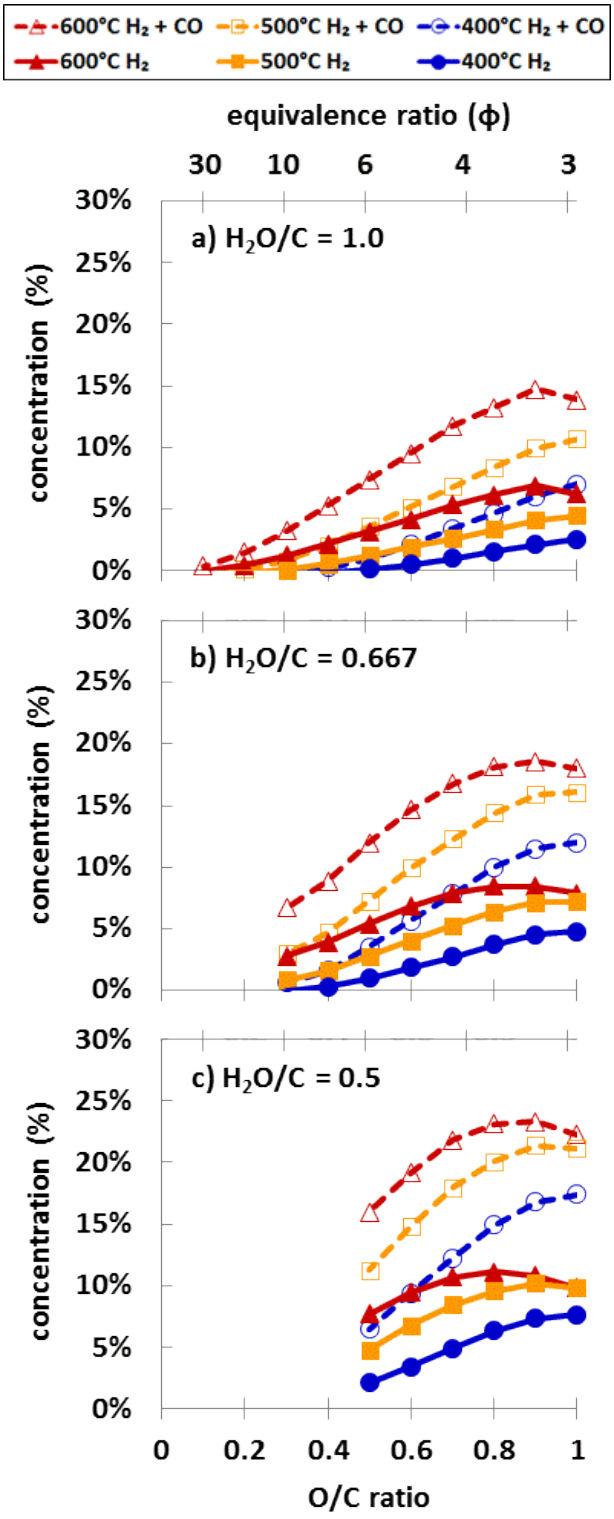

Figure 14. Hydrogen and reformate production during partial oxidation reforming of gasoline in the presence of water vapor at S/C ratios of a) 1.0, b) 0.667, and c) 0.5.

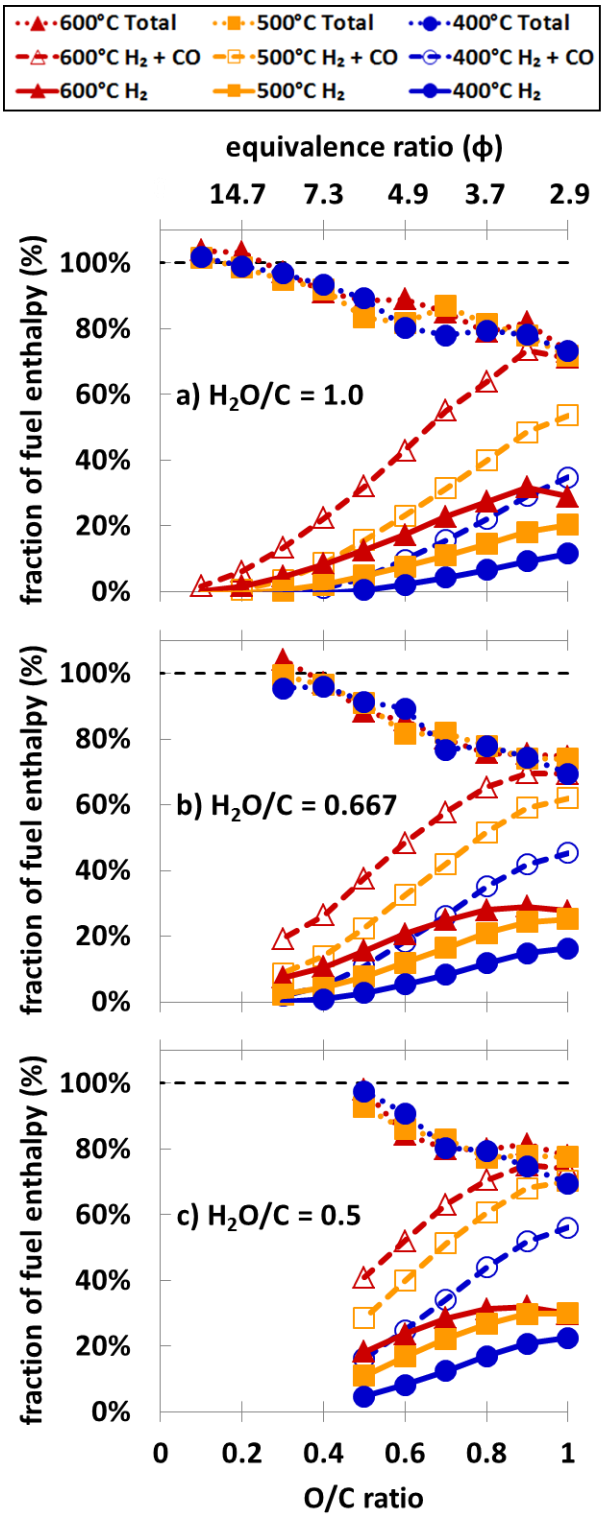

Figure 15. Fraction of fuel enthalpy recaptured during partial oxidation reforming of gasoline in the presence of water vapor at S/C ratios of a) 1.0, b) 0.667, and c) 0.5.

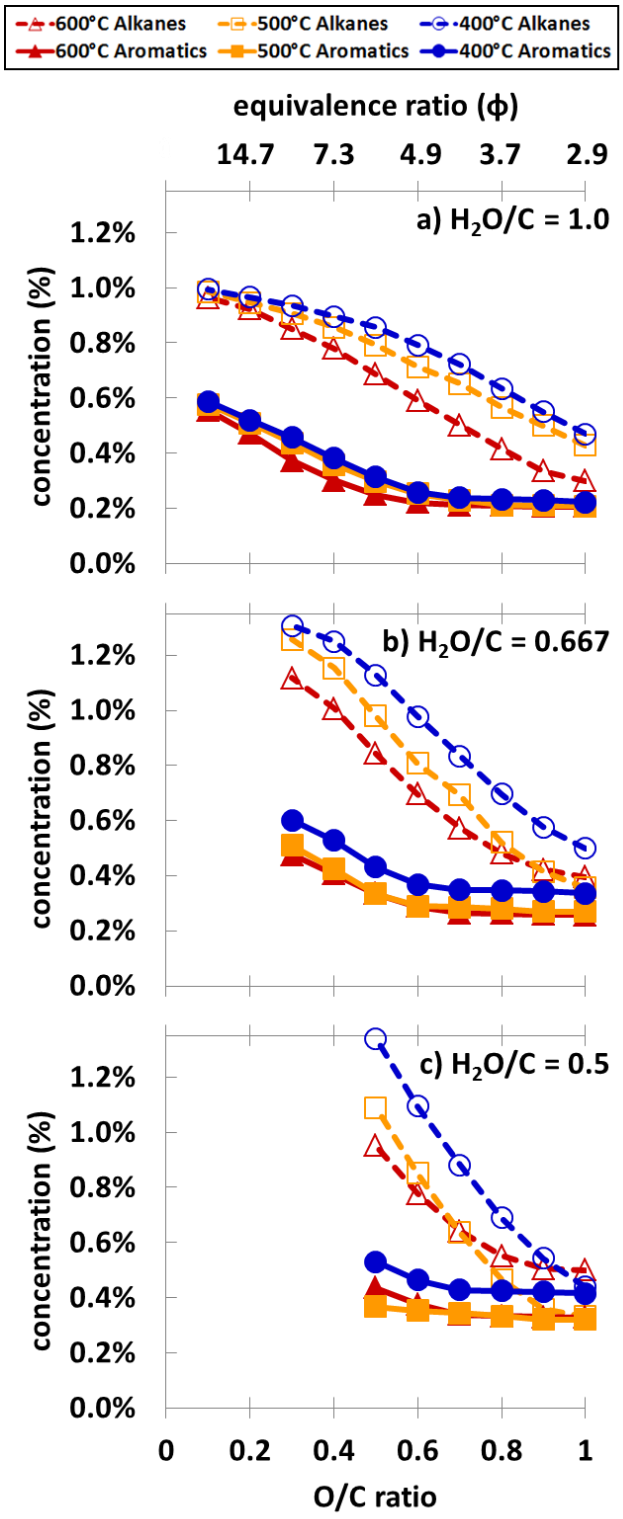

Figure 16. Concentration of alkanes and aromatics during partial oxidation reforming of gasoline in the presence of water vapor at S/C ratios of a) 1.0, b) 0.667, and c) 0.5.

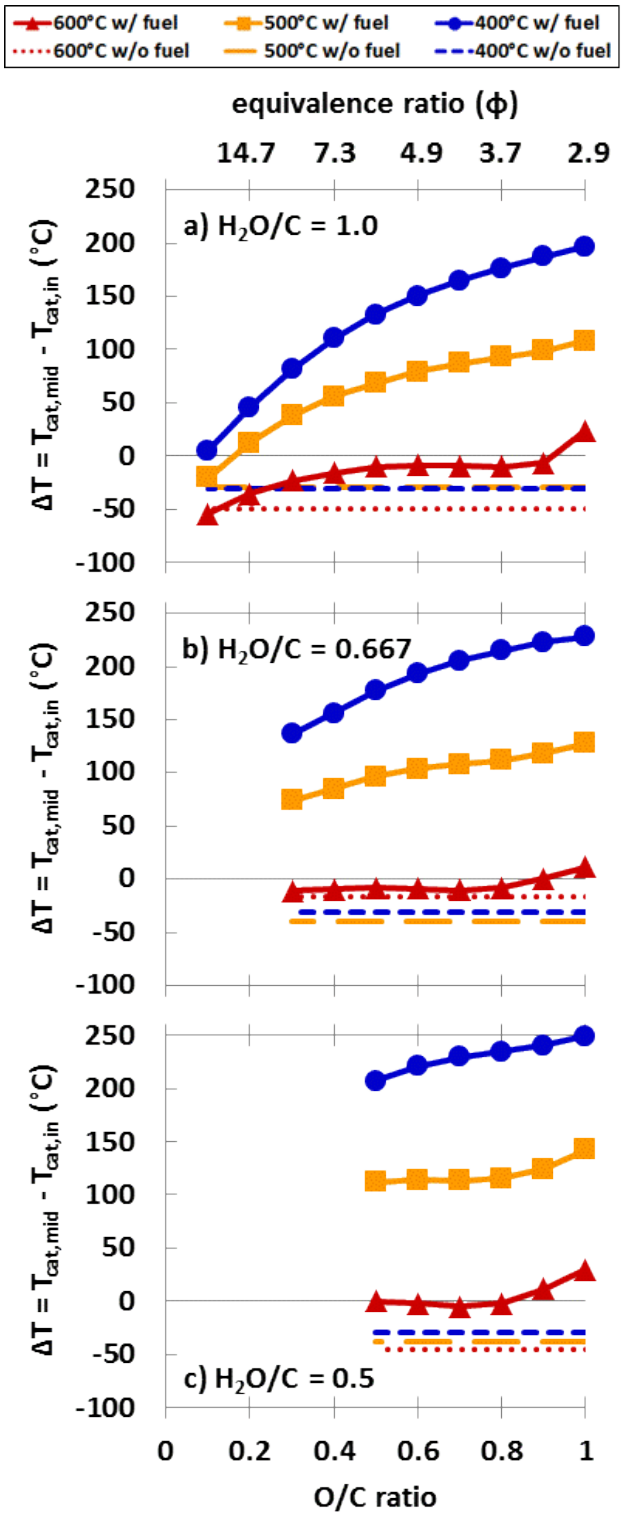

Figure 17. Temperature change from inlet to midpoint of catalyst during partial oxidation reforming of gasoline in the presence of water vapor at S/C ratios of a) 1.0, b) 0.667, and c) 0.5.